DOE/ET/15492--T12

R8

APT PR 4

AIR POLLUTION TECHNOLOGY, INC.

LABORATORY/BENCH-SCALE TESTING AND
EVALUATION OF A.P.T. DRY-PLATE SCRUBBER

TECHNICAL PROGRESS REPORT

for the period December 1, 1980 through February 28, 1981

Fourth Quarterly Progress Report

DOE Contract DE-AC01-80ET15492

March 30, 1981

4901 MORENA BLVD., SUITE 402 SAN DIEGO, CA 92117 (714) 272-0050

DISCLAIMER

FOURTH QUARTERLY TECHNICAL PROGRESS REPORT FOR: TESTING AND EVALUATION OF THE A.P.T. DRY-PLATE SCRUBBER

DE-AC21-90ET15492

INTRODUCTION

The A.P.T. Dry Plate Scrubber (DPS) uses a shallow, dense mobile bed of solid collector granules which move across a perforated plate. The gas stream containing fine particles and vapors is moved upward through the perforations to form high velocity gas jets. The fine particles are removed by inertial deposition onto the collector granules or by direct interception. Electrostatic forces also can be used to improve the collection efficiency and increase the adhesive forces between the particles and collectors.

The DPS column consists of a series of collection stages (perforated plates) with the collectors either passing sequentially over each stage or being fed separately to each stage. The stages can be designed so as to promote the collection of large particles on the lower stages and the collection of fine particles and alkali vapors on the upper stages.

The DPS is especially well suited for cleaning high temperature and pressure gases such as the effluent from a pressurized fluidized bed combustion (PFBC) process. The objective of this project is to conduct a bench scale experimental evaluation of the DPS at high temperature and pressure to determine its potential for controlling particulate and alkali vapor emissions from PFBC processes.

Approach

This project is divided into two phases and seven major tasks as listed in Table 1. Phase I is a preliminary study consisting of a theoretical review, preliminary particle collection experiments and preliminary alkali sorption experiments. The purpose of Phase I is to provide specific design criteria for Phase II.

Phase II is a bench scale evaluation of the DPS at high temperature (900°C) and pressure (100 kPa). The bench scale DPS will be designed and evaluated for both particulate and alkali vapor control. The results will be used to develop an engineering design model for predicting the efficiency and power costs for the DPS. A detailed process design of a DPS sub-pilot plant installed at a PFBC facility will be made. The process economics will be evaluated in terms of capital and operating costs as a function of cleaning efficiency.

TABLE 1. WORK BREAKDOWN STRUCTURE

Task 1.0		THEORETICAL STUDY
	1.1	Literature Review
	1.2	Calculations
Task 2.0		PRELIMINARY PARTICLE EXPERIMENTS
	2.1	Single Stage DPS
	2.2	Electrostatic DPS
	2.3	Multiple Stage DPS
Task 3.0		PRELIMINARY ALKALI EXPERIMENTS
	3.1	Sorbent Screening
	3.2	Sorbent Capacity and Efficiency
	3.3	Sorbent Attrition
Task 4.0		HIGH TEMPERATURE AND PRESSURE EXPERIMENTS
	4.1	Design and Construction
	4.2	Simulated PFBC Experiments
	4.3	AFBC Experiments
Task 5.0		DESIGN MODEL
Task 6.0		PROCESS DESIGN
Task 7.0		FINAL REPORT

TECHNICAL OBJECTIVES FOR THIS REPORTING PERIOD

The principal technical objectives for this quarter are listed below:

Task 2.3 - Multiple Stage DPS Experiments

1. Complete optimization tests on three-stage DPS.
2. Complete experiments on three-stage continuous EDPS with electrostatic augmentation.
3. Conduct experiments to measure electrical conductivity of alumina collector bed at temperatures up to 800°C.
4. Estimate required performance.

Task 3.1 - Sorbent Screening Experiments

1. Complete initial screening evaluation of potential sorbent materials.
2. Select sorbent (or sorbents) for further evaluation and testing.

Task 3.2 - Sorbent Capacity, Rate and Efficiency

1. Complete fabrication of test apparatus.
2. Test the flame photometer for high temperature air sampling.
3. Carry out sorption runs with diatomaceous earth and activated bauxite at 900°C in single stage DPS.
4. Investigate pretreatment methods for sorbents.

Task 4.1 - High Temperature and Pressure Bench Scale DPS

1. Complete conceptual process design for bench scale DPS.
2. Begin experiments to study downcomer configurations.

Task 4.3 - Bench Scale Tests on AFBC System

1. Complete conceptual design modifications for AFBC system.
2. Begin renovating AFBC plant.

TECHNICAL PROGRESS

TASK 2.3 - MULTIPLE STAGE DPS EXPERIMENTS

The preliminary particle collection experiments have been completed. The ranges of experimental parameters are summarized in Table 2. Results of the experiments run during this quarter are discussed below.

Optimization Tests for Three-Stage DPS

Tests were continued in December to optimize the design parameters for the 3-stage DPS for fine particle control. Parameters that were studied include superficial velocity, jet velocity, bed depth, collector mass flow rate, and collector material. The experimental setup is illustrated in Figure 1. In order to study a wider range of collector flow rates with better control, we used the multiple feed configuration with collectors fed separately to each stage. The experimental conditions are summarized in Table 3. All experiments were run with plate H which has the largest % open area of the plates we have used (see Table 4). Runs 10/P1-10/P3 used alumina collectors. Runs 10/P4-10/P8 used zirconia beads. The properties of all collector materials used are listed in Table 5.

Data for Runs 10/P1 and 10/P2 are presented in Figure 2. For comparison, data from last month's Run 9/P11 are also shown. Runs 9/P11 and 10/P1 were run at the same superficial velocity and different jet velocities. The higher jet velocity (19.2 cm/s for Run 9/P11) was more efficient at collecting fine particles. These data are consistent with earlier runs which indicate that the efficiency increases with jet velocity up to about 19 m/s. Above 19 m/s, reentrainment problems begin and the overall collection efficiency decreases.

Reentrainment can result either from too high a jet velocity (high impact energy) or from excessive bed movement (superficical velocity too high). This effect of superficial velocity may be seen in Figure 2 by comparing Runs 9/P11 and 10/P2. These runs used the same jet velocity and different superficial velocities (48 cm/s and 68 cm/s). The higher superficial velocity (Run 10/P2) showed much worse collection efficiency.

TABLE 2. SUMMARY OF EXPERIMENTAL PARAMETERS

TEST PARAMETER	RANGE TESTED	OPTIMUM RANGE	COMMENTS
1. Gas Superficial Velocity, cm/s	25-80	45-50 (A.S. beads) 70-75 (Zircon beads)	Refer Table 5, No. 4 Refer Table 5, No. 12
2. Gas Jet Velocity, m/s	15-60	18-20 (A.S. beads) 28-30 (Zircon beads)	Refer Table 5, No. 4 Refer Table 5, No. 12
3. Support Jet Plate			
3.1 % Open Area, %	1.0-4.0	2.50	
3.2 Jet Diameter, mm	1.0-1.6	1.20	
3.3 Geometry	square, triangular	square	Not significant effect of the two geometries tested
3.4 C-C Spacing, mm	6.0-11.0	6.5	
4. Collector Materials -	Refer Table 5 for details		
Materials	Refer Table 5	No. 4, 5, 12 (Table 1)	Suitable for HTP applications
Diameter, mm	0.40-1.20	0.6-1.0	
5. Static Bed Height, cm	0.50-3.0	1.50	
6. Collector Feed Rate: Mass of Collectors/ Mass of Gas (ratio)	0.1:1.0 to 1:1	0.5 - 0.7 kg collectors per kg of gas	
7. Electrostatic Conditions:			
7.1 (a) Particle Charger, kV /cm	-5.4 (D.C.)		
(b) Polarization, kV /cm	-4.5 (D.C. & Co-flow)		

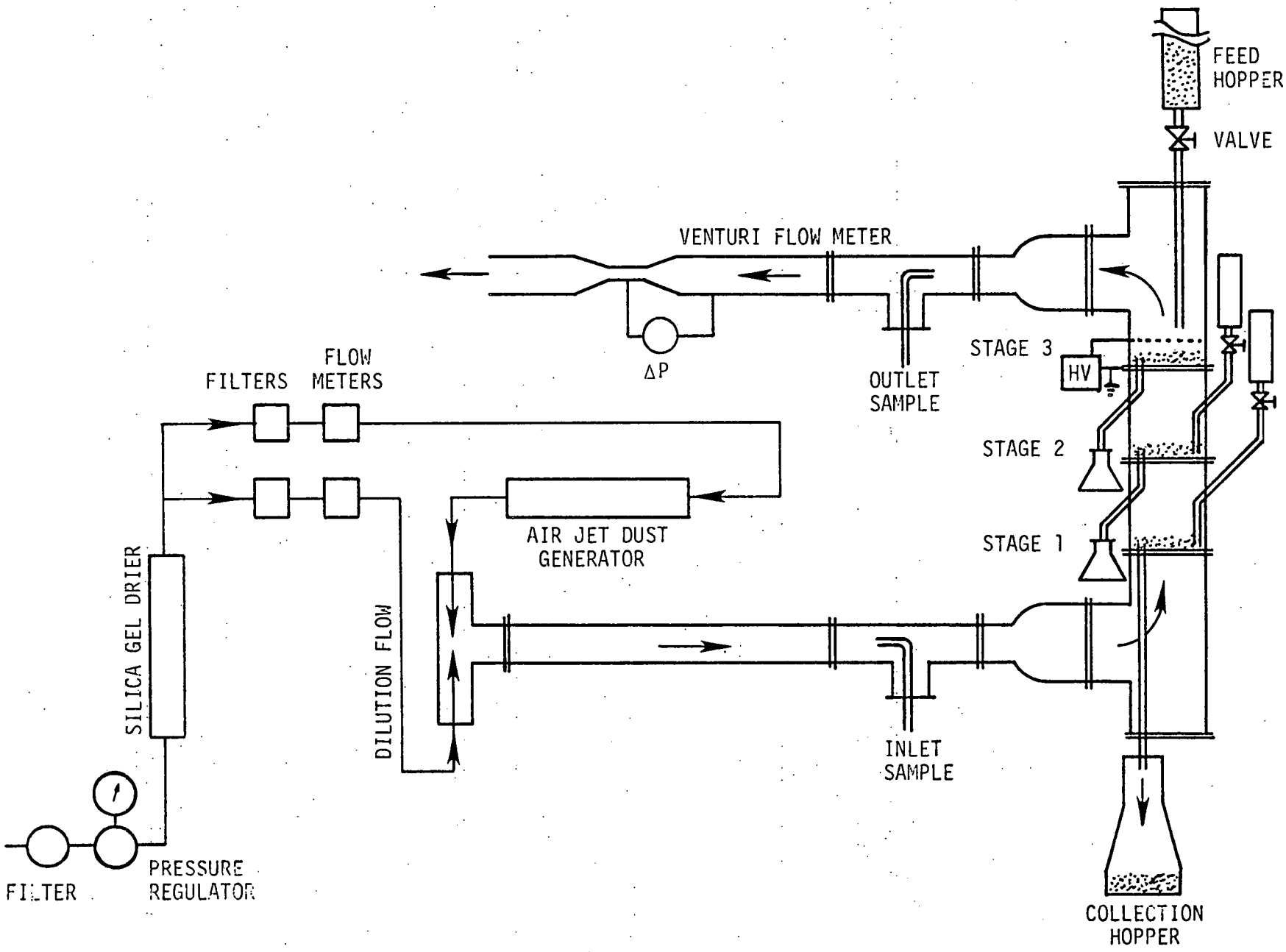

Figure 1. Schematic diagram of three-stage continuous dry plate scrubber with multiple collector feed.

TABLE 3. SUMMARY OF EXPERIMENTAL CONDITIONS FOR THREE STAGE DRY PLATE SCRUBBER (TEST AEROSOL: REDISPERSED FLY ASH)

Rm No.	Q_G m^3/min	u_s cm/s	u_j, m/s Stage No. 1	2	3	ΔP_{bed}, cm W.C. Stage No. 1	2	3	Bed Ht., cm Stage No. 1	2	3	Mass Flow Rate, g/s Collector (Total)	Gas	Inlet Part. conc., mg/m^3	Plate No. Stage 1	2	3	Collector Bed Material	Collector Feed Mode
10/P1	0.23	48.0	13.5	13.5	13.5	4.1	4.6	4.6	1.5	1.5	1.5	16.2	4.7	1,600	H	H	H	Alumina	Individual
10/P2	0.33	68.1	19.2	19.2	19.2	4.8	4.8	4.8	1.5	1.5	1.5	8.8	6.7	1,056	H	H	H	"	"
10/P3	0.25	51.2	14.4	14.4	14.4	6.1	6.1	6.4	2.5	2.5	2.5	8.8	5.0	885	H	H	H	"	"
10/P4	0.25	51.2	14.4	14.4	14.4	4.8	5.1	5.1	1.5	1.5	1.5	8.2	5.0	1,428	H	H	H	Zirconia	"
10/P5	0.28	57.3	16.1	16.1	16.1	5.1	5.1	5.1	1.5	1.5	1.5	5.7	5.6	2,068	H	H	H	"	"
10/P6	0.25	51.2	14.4	14.4	14.4	5.1	5.1	5.1	1.5	1.5	1.5	12.3	5.0	2,242	H	H	H	"	"
10/P7	0.25	51.2	14.4	14.4	14.4	5.1	5.1	5.1	1.5	1.5	1.5	14.0	5.0	3,123	H	H	H	"	"
10/P8	0.25	51.2	14.4	14.4	14.4	5.1	5.1	5.1	1.5	1.5	1.5	19.8	5.0	4,128	H	H	H	"	"

TABLE 4. SUPPORT JET PLATE DATA

Plate Thickness = 0.32 cm

Plate Diameter = 10.20 cm

Plate No.	Jet Dia., mm	No. of Jets	% Open Area	Pattern (C-C Spacing*, mm)
1	1.0	216	2.05	Square (6.0)
2.	2.0	104	4.00	Square (8.0)
3.	1.6	120	2.93	Square (8.0)
4.	1.2	220	3.02	Square (6.0)
5.	1.2	68	0.93	Square (11.0)
6.	1.0	108	1.03	Square (8.0)
7.	1.2	120	1.65	Square (8.0)
A	1.2	112	1.54	Square (8.0)
B	1.2	106	1.45	Square (8.0)
C	1.2	114	1.56	Square (8.0)
D	1.2	116	1.60	Square (8.0)
E	1.2	99	1.36	Square (9.0)
F	1.2	145	2.00	Square (7.5)
G	1.2	182	2.50	Square (6.5)
H	1.6	145	3.50	Triangular (7.5)
J	1.4	145	2.75	Triangular (7.5)
K	1.2	145	2.00	Triangular (7.5)
L	1.6	111	2.75	Triangular (8.0)

*C-C spacing is the distance from center to center of two adjacent jets

TABLE 5. SUMMARY OF COLLECTOR MATERIAL SPECIFICATIONS

	Material	Mean Diameter, mm	Diameter Range, mm	True Density, g/cm^3	Bulk Density, g/cm^3	umf cm/s	Shape
1.	Alumina Spheres	0.50	Uniform Size	3.86	2.40	30.0	Spherical
2.	Alumina Spheres	0.65	Uniform Size	1.90	1.10	23.0	Spherical
3.	Alumina Spheres	0.83	Uniform Size	1.90	1.00	34.0	Spherical
4.	Alumina Spheres	0.68	0.42 - 0.84	3.60	2.20	43.0	Spherical*
5.	Alumina Spheres	1.00	0.84 - 0.12	3.60	____	____	Spherical*
6.	Glass Beads	0.48	0.45 - 0.50	2.90	1.80	23.0	Spherical
7.	Glass Beads	1.0	Uniform Size	2.50	1.53	54.0	Spherical
8.	Nickel Spheres	0.68	0.42 - 0.84	8.50	5.26	98.0	Spherical
9.	Nickel Spheres	0.38	0.30 - 0.60	8.50	5.12	39.0	Spherical
10.	S.S. 316 Shot	0.58	0.50 - 0.70	7.50	____	____	Round with rough edges
11.	Zircon Beads (ZrO_2)	0.38	0.30 - 0.60	5.40	3.10	____	Ellipsoidal**
12.	Zircon Beads (ZrO_2)	0.68	0.42 - 0.84	5.40	3.20	59.0	Ellipsoidal**

*Commercially available material ($0.4 - 0.8/lb.)

**Special order required ($8.0 - 9.0/lb.)

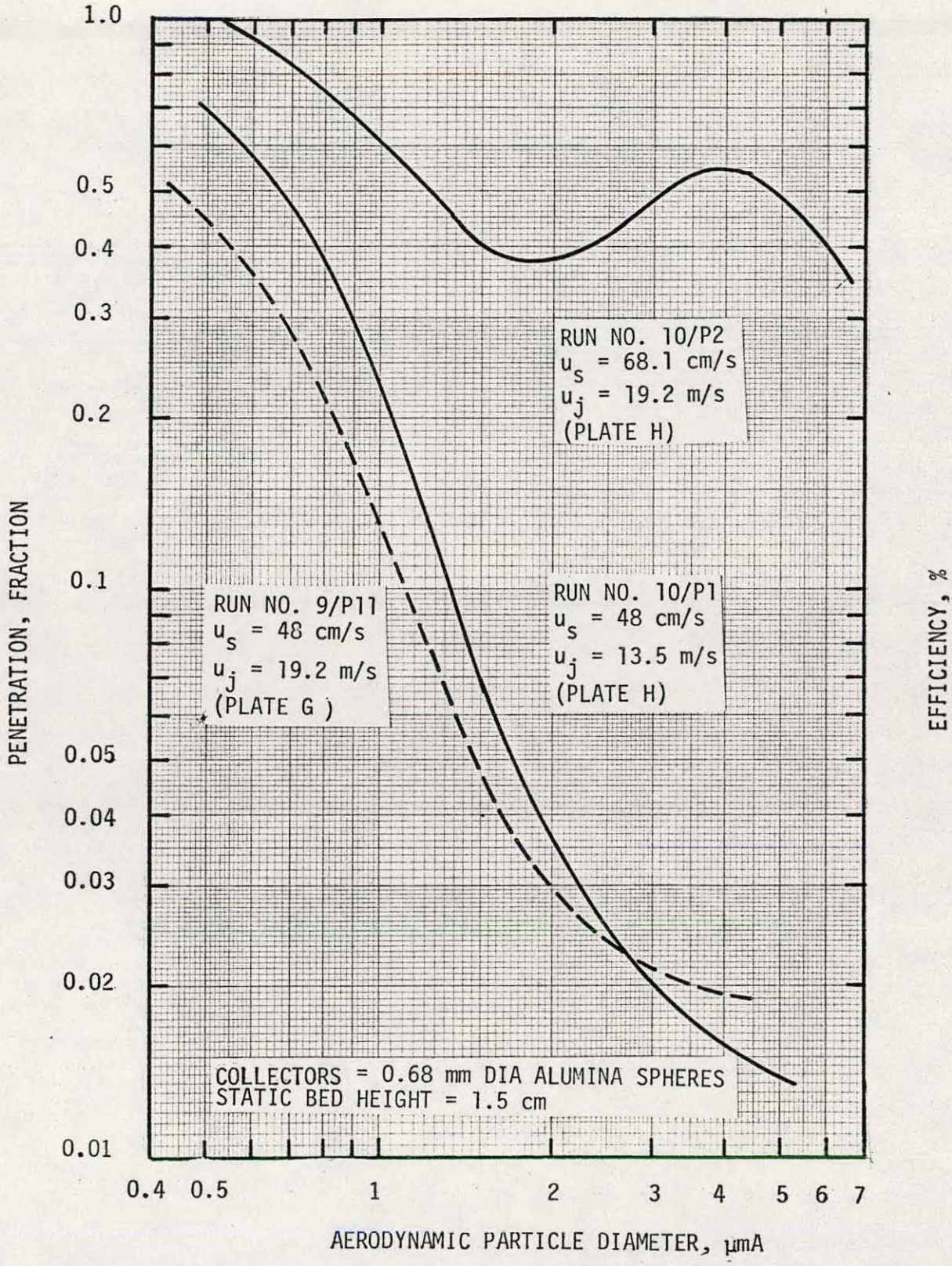

Figure 2. Superficial and jet velocity effects on DPS collection efficiency.

In general, we have not been able to operate at superficial velocities higher than about 50 cm/s without reentrainment problems. We are looking at various jet patterns and jet diameters to see if we can optimize the jet plate design for maximum efficiency and superficial velocity (gas capacity). Denser collectors such as zirconia beads are also being tested and preliminary results look promising.

An attempt was made to increase the superficial velocity (and hence gas capacity) by increasing the static bed height from 1.5 cm to 2.5 cm. The results are shown in Figure 3. The higher flow rate, deeper bed data (Run 10/P3) show more penetration (lower collection efficiency) and thus worse performance.

Figure 3 also presents data for zirconia collectors at a gas flow rate of 250 ℓ/min. The zirconia collectors are denser than the alumina spheres so it may be possible to operate the system at a higher flow rate while keeping the degree of bed movement the same as achieved using alumina at a lower flow rate. This effect is shown in Figure 3. Zirconia beads achieve better efficiency, at 60% lower collector volume feed rate (7% lower mass feed rate) than alumina beads. However, these zirconia collectors are smaller than the alumina (see Table 5). Larger zirconia beads (0.5 - 0.85 mm) have just beed received and will be tested next month.

The major problem with zirconia beads is that they seem to break up by attrition as they are reused. Runs 10/P5 through 10/P8 were run at various collector feed rates to see if we could reduce this attrition problem. The collectors were washed, dried and recycled for each run. They were visibly worn down more each run and no clear improvement was observed.

Electrostatic Three-Stage DPS (EDPS)

The laboratory 3-stage DPS was modified to study electrostatic augmentation of the system. The experimental setup is illustrated in Figure 4. The major modifications are:

1. A corona discharge particle precharger was installed upstream from the inlet sample probe.

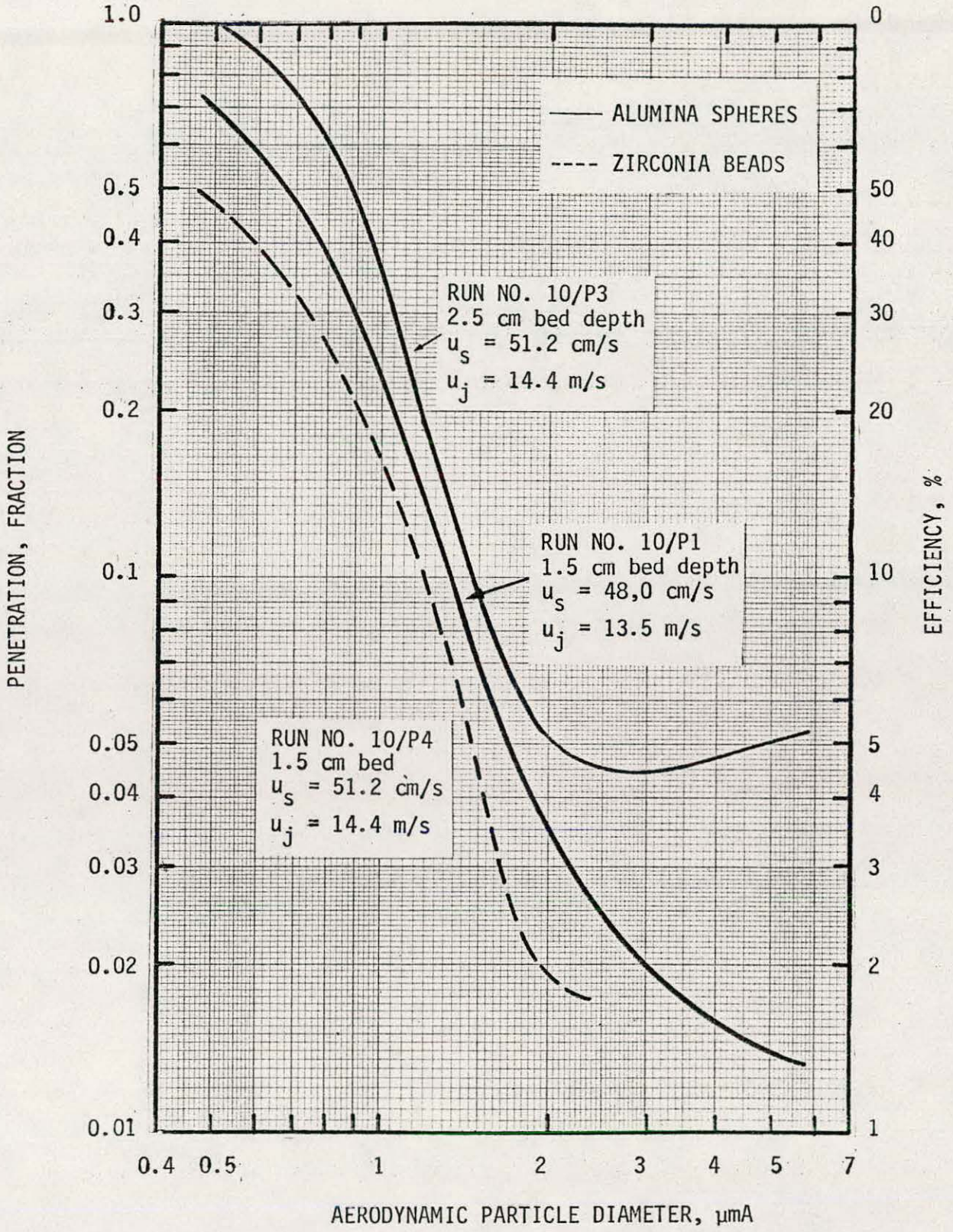

Figure 3. Effects of DPS static bed height, collector material, and gas capacity.

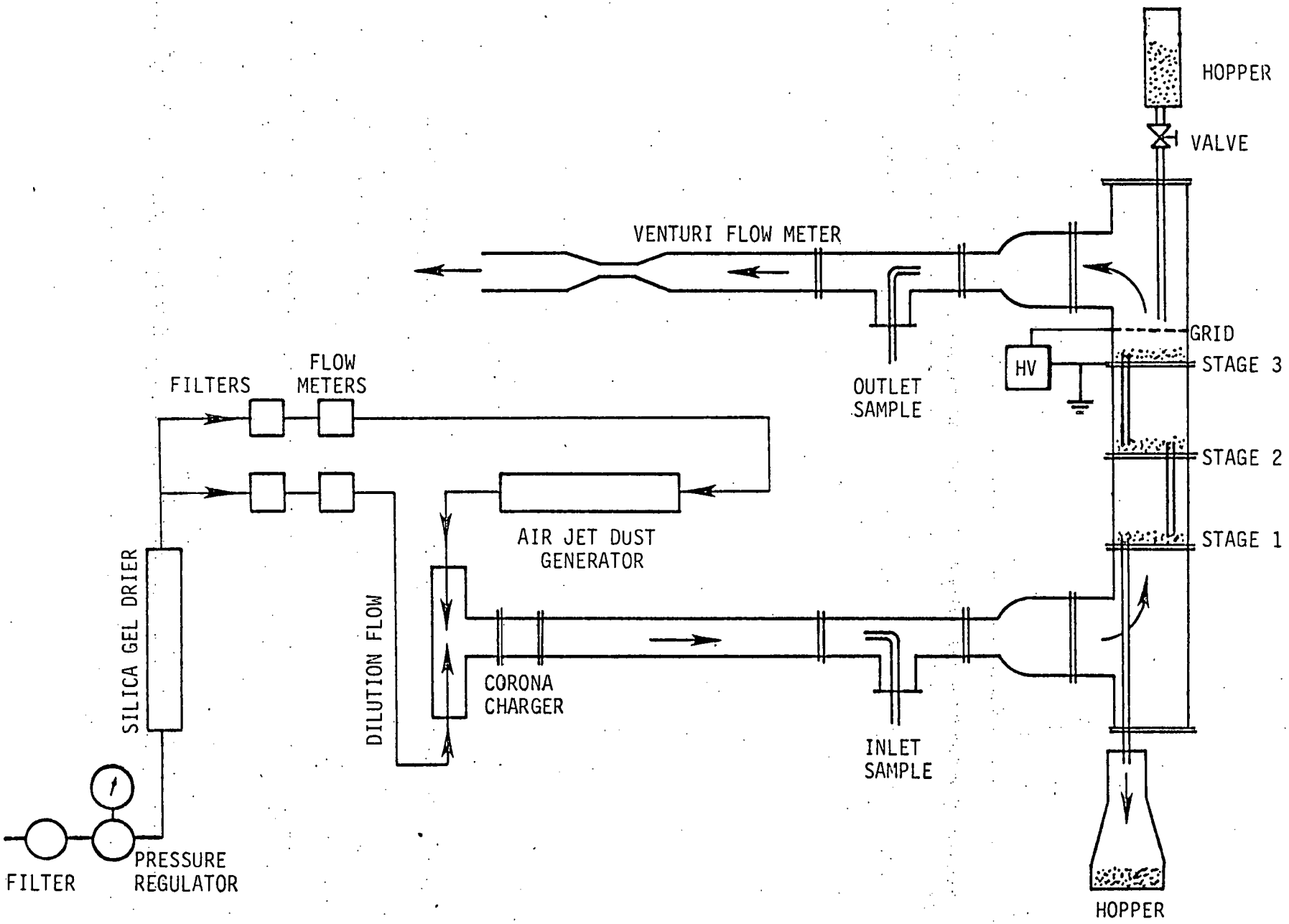

Figure 4. Schematic diagram of three-stage continuous dry plate scrubber with single collector feed.

2. An electrically isolated screen was installed above the third jet plate and was attached to the high voltage power supply. The third jet plate was grounded.

Nineteen EDPS runs were made in December. Table 6 summarizes the test conditions for these runs. High density alumina spheres were used as collectors. The test dust was redispersed fly ash.

Figures 5 through 7 compare typical experimental penetration data for the 3-stage DPS and 3-stage EDPS. Figure 8 compares 3-stage data with 2-stage data. The following abbreviations are used:

UP/NC - uncharged particles, neutral collectors
CP/PC - charged particles, polarized collectors

It should be noted that for the 3-stage and 2-stage EDPS data, the top stage has the electric field (CP/PC) and the lower stages have no field but particles are charged (CP/NC). For simplicity we will use the abbreviation "CP/PC" to indicate the charged/polarized conditions for the multiple stage EDPS.

All the efficiency data for the EDPS show considerable improvement for particle diameters smaller than 2 μmA. Above 2 μmA the electrostatic forces have little influence and the curves flatten out or increase. It may be that leveling off in efficiency is a result of reentrainment. This is being looked into more closely.

TABLE 6. SUMMARY OF TEST CONDITIONS OF CONTINUOUS ONE-, TWO- AND THREE-STAGE EDPS
(COLLECTORS: ALUMINA SPHERES)

Rn No.	Q_G m^3/min	u_s cm/s	u_j, m/s Stage No. 1	2	3	ΔP_{bed}, cm W.C. Stage No. 1	2	3	Bed Ht., cm Stage No. 1	2	3	Mass Flow Rate, g/s Collector	Gas	Inlet conc., mg/m^3	Plate No. Stage 1	2	3	Electrostatic Conditions
4/11/P3	0.22	44.5	17.8	--	--	6.4	--	--	1.5	--	--	3.3	4.4		G	-	-	CP/PC**
4/11/P4	0.22	44.5	17.8	--	--	6.4	--	--	1.5	--	--	3.3	4.4		G	-	-	UP/NC**
4/11/P5	0.22	44.5	17.8	--	--	6.4	--	--	1.5	--	--	3.3	4.4		G	-	-	CP/PC**
4/11/P6	0.22	44.5	16.2	16.2	16.2	5.8	5.8	5.8	1.5	1.5	1.5	3.3	4.4	687	J	J	J	CP/PC**
4/11/P7	0.22	44.5	16.2	16.2	16.2	5.8	5.8	5.8	1.5	1.5	1.5	3.3	4.4	--	J	J	J	CP/PC**
4/11/P8	0.22	44.5	16.2	16.2	16.2	5.8	5.8	5.8	1.5	1.5	1.5	3.3	4.4	2567	J	J	J	UP/NC**
4/11/P9	0.23	48.0	17.5	17.5	17.5	6.0	6.0	6.0	1.5	1.5	1.5	3.3	4.7	491	J	J	J	CP/PC**
4/11/P10	0.23	48.0	17.5	17.5	17.5	6.0	6.0	6.0	1.5	1.5	1.5	3.3	4.7	197	J	J	J	CP/PC**
4/11/P12	0.34	70.0	28.0	28.0	28.0	11.4	11.4	11.7	1.5	1.5	1.5	7.2	6.8	412	G	G	G	CP/PC*
4/11/P13	0.34	70.0	28.0	28.0	28.0	11.4	11.4	11.7	1.5	1.5	1.5	7.2	6.8	637	G	G	G	CP/PC*
4/11/P14	0.34	70.0	28.0	28.0	28.0	11.4	11.4	11.7	1.5	1.5	1.5	7.2	6.8	573	G	G	G	CP/PC*
4/11/P15	0.34	70.0	28.0	28.0	28.0	11.4	11.4	11.7	1.5	1.5	1.5	7.2	6.8	670	G	G	G	CP/PC*
4/11/P16	0.34	70.0	28.0	28.0	28.0	11.4	11.4	11.7	1.5	1.5	1.5	7.2	6.8	680	G	G	G	CP/PC*
4/11/P17	0.34	70.0	28.0	28.0	28.0	11.4	11.4	11.7	1.5	1.5	1.5	7.2	6.8	799	G	G	G	UP/NC*
4/11/P18	0.22	44.5	17.8	17.8	17.8	5.8	6.4	6.8	1.5	1.5	1.5	3.3	4.4	1378	G	G	G	CP/PC**
4/11/P19	0.22	44.5	17.8	17.8	17.8	5.8	6.4	6.8	1.5	1.5	1.5	3.3	4.4	3522	G	G	G	CP/PC**

* ZIRCON BEADS: 0.42-0.85 mm DIA
$\rho = 5.4 g/cm^3$

** ALUMINA SPHERES: 0.42-0.85 mm DIA.
$\rho = 3.6 g/cm^3$

PARTICLE: REDISPERSED FLY ASH
PARTICLE CHARGING FIELD STRENGTH: - 5.4kV/cm
POLARIZATION FIELD STRENGTH: - 4.5kV/cm

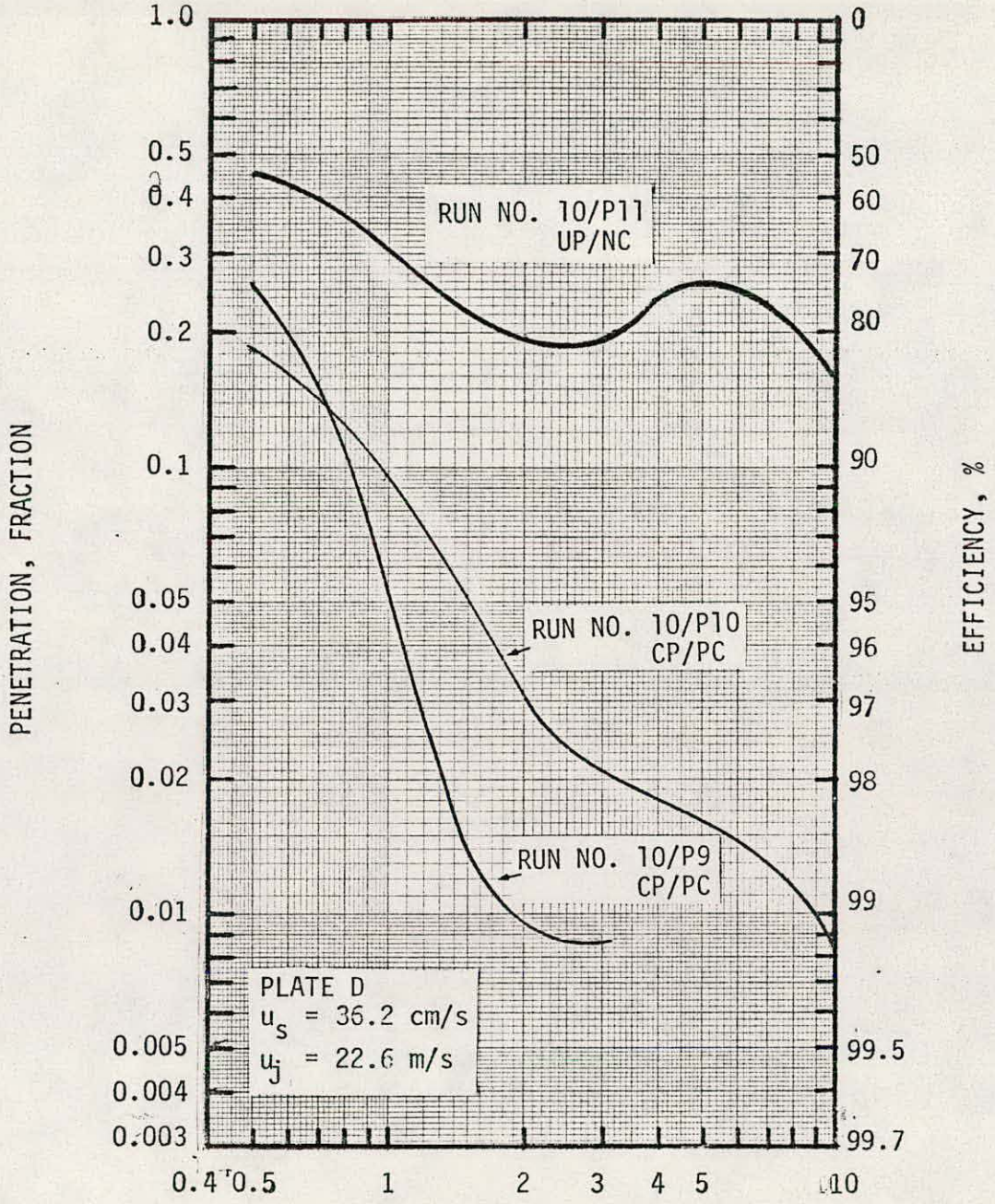

Figure 5. Measured three-stage continuous EDPS performance.

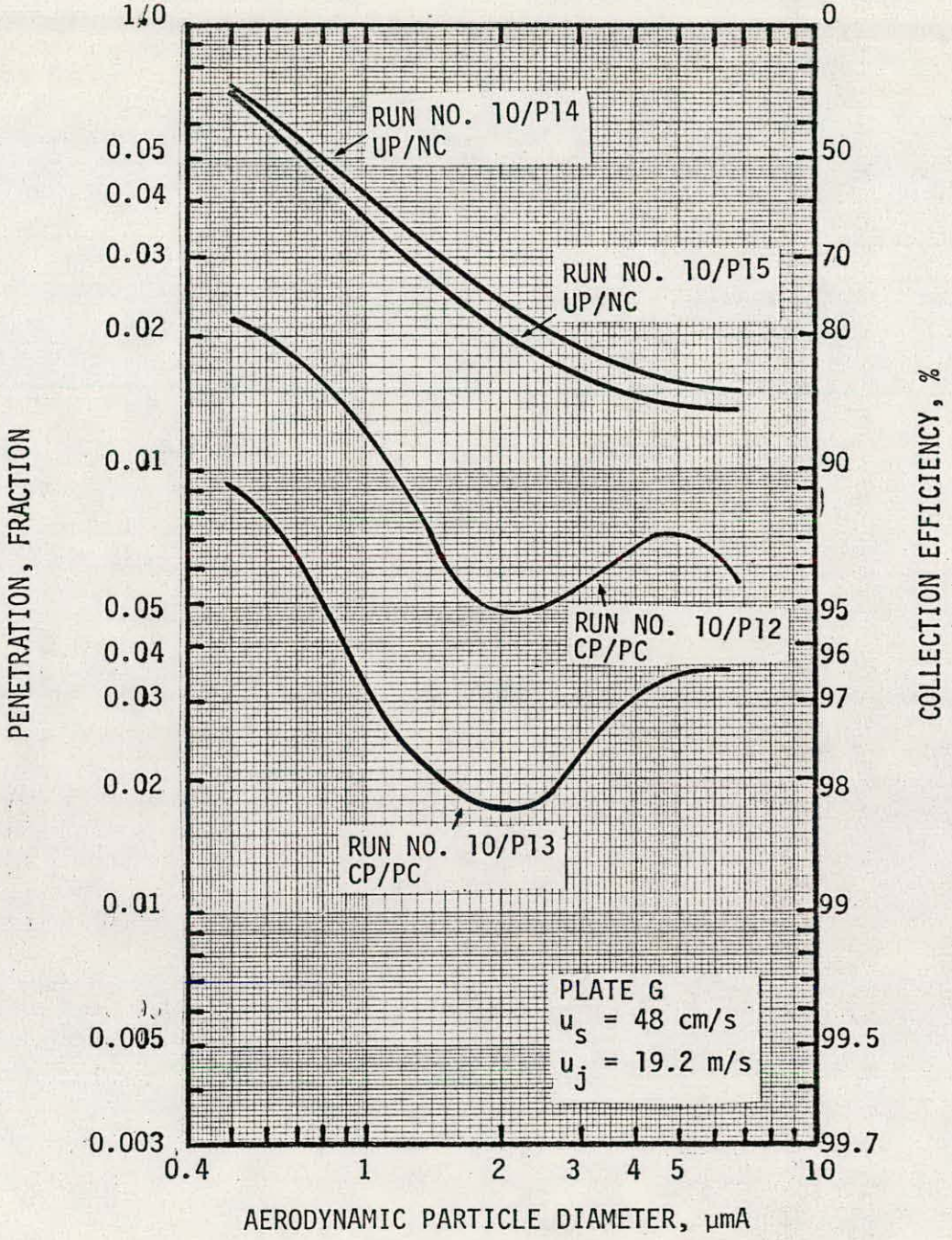

Figure 6. Measured three-stage EDPS performance.

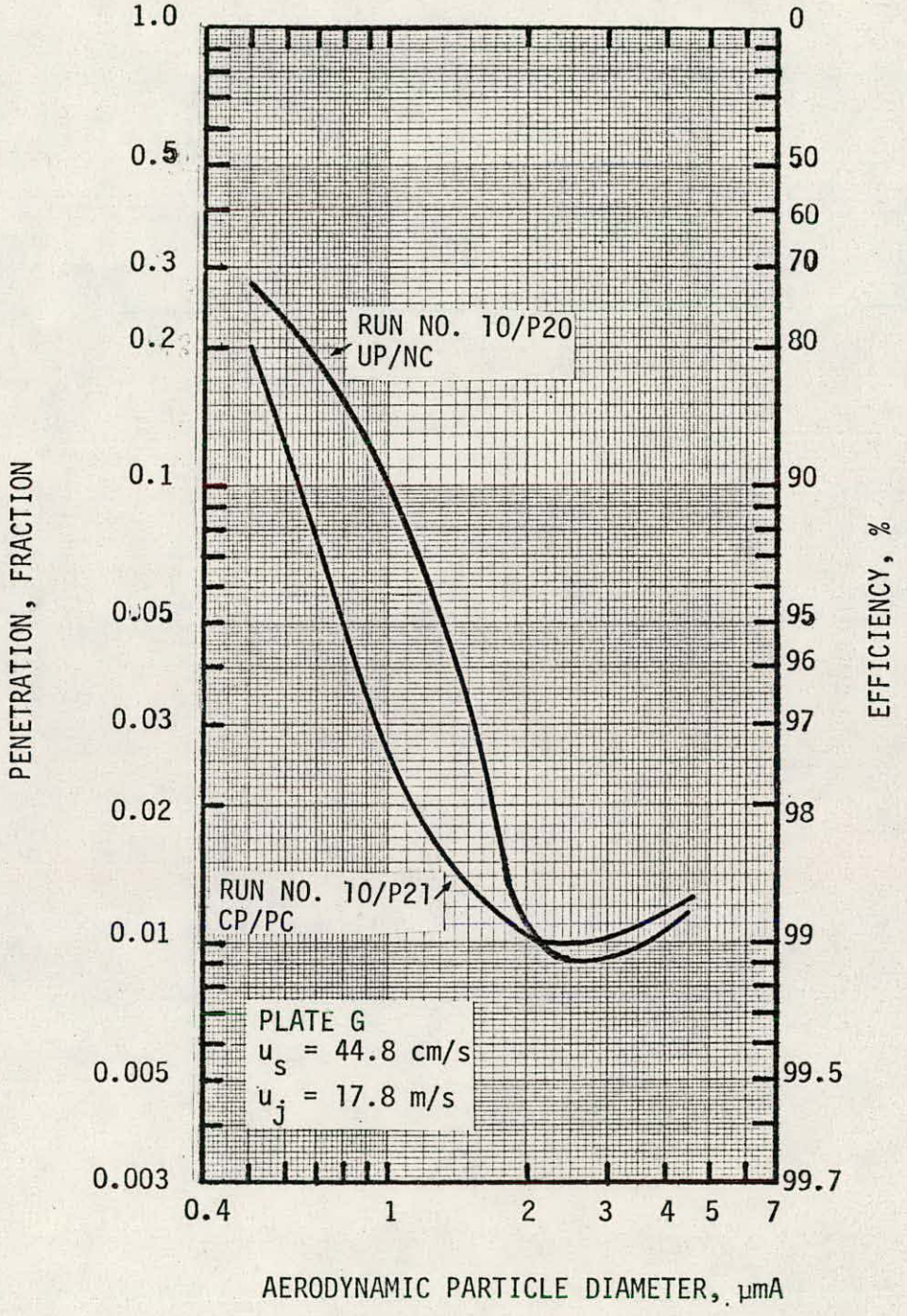

Figure 7. Measured three-stage EDPS performance.

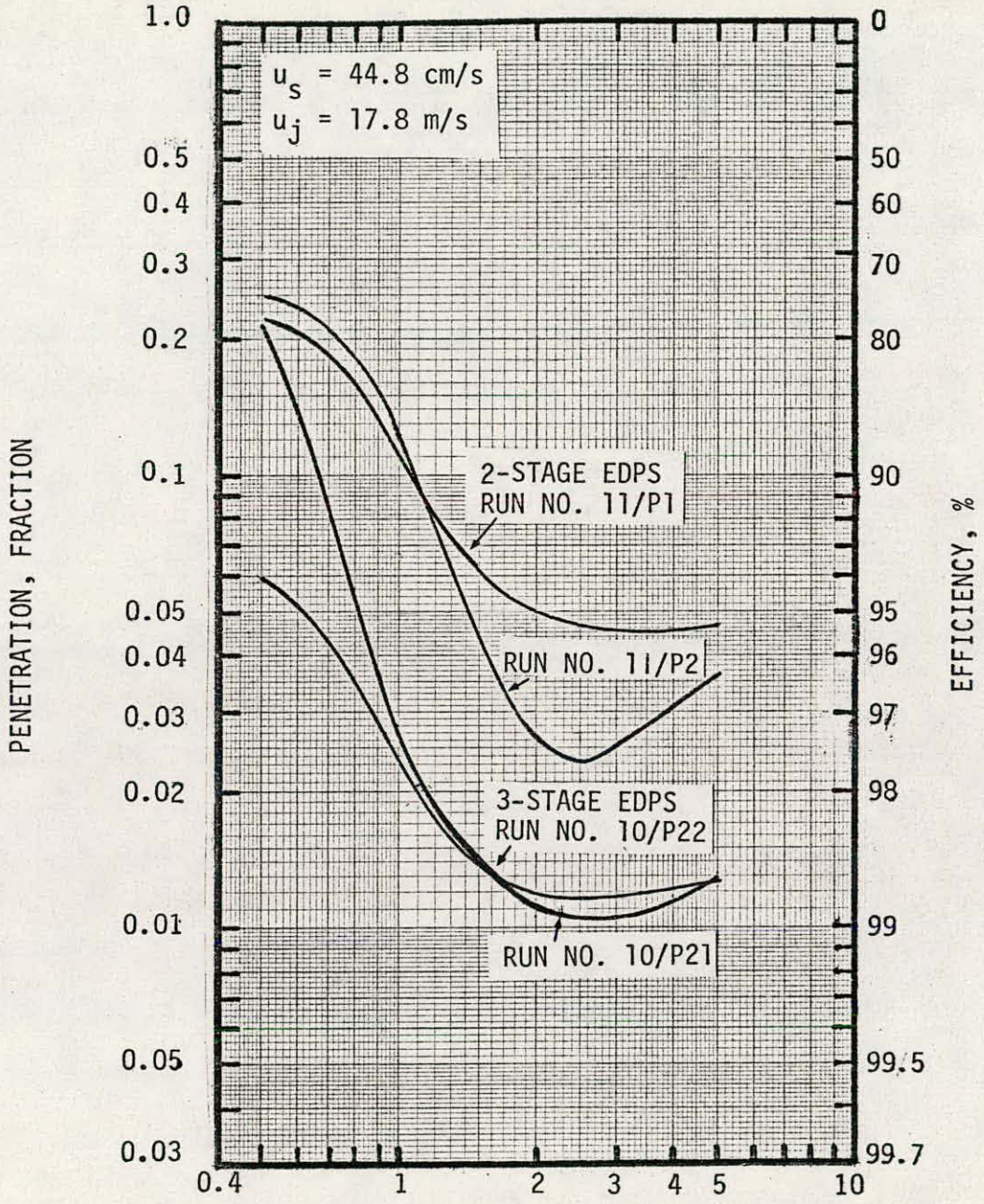

Figure 8. Measured three-stage and two-stage EDPS performance.

Sixteen EDPS runs were carried out in January. Table 7 summarizes the test conditions for these runs.

a) Single-, Two- and Three-Stage Continuous EDPS

Runs 11/P3-11/P5 were made on the single-stage continuous system. Measured grade penetration results for these runs are presented in Figure 9. The single stage data are compared with 2- and 3- stage experimental data in Figure 10.

Efficiency data for the continuous EDPS show larger improvement from two-stage or three-stage system as compared to that of from single-stage and two-stage. This is a result of the electric field applied across Stage 3.

b) Jet Plate Geometry

Runs 11/P6-11/P10 used jet geometry #J which has a larger jet diameter (higher percent open area) than that of the geometry #G. The design data of these plate geometries are tabulated in Table 4. Figure 11 compares the performance results for these two plate geometries. Excessive bed movement was observed with plate #J resulting in higher penetration (lower collection efficiency). Jet plate #G has given the best performance of the plates tested.

c) Zirconia Beads as Collector Granule

Zirconia beads, with physical properties as listed in Table 5, were used as collectors. The zirconia are denser than the alumina spheres, therefore it was possible to operate the system at a higher gas velocity (u_s = 70 cm/s and u_j = 28 m/s) while keeping the degree of bed movement the same as achieved using alumina spheres at a lower gas velocity (u_s = 44.5 m/s and u_j = 17.8 m/s).

Figure 12 presents performance data with zirconia collectors for the electrostatic DPS (EDPS) and neutral DPS. The EDPS is clearly more efficient.

TABLE 7. SUMMARY OF EXPERIMENTAL CONDITIONS FOR CONTINUOUS, THREE-STAGE ELECTROSTATIC DPS (COLLECTORS: ALUMINA SPHERES PARTICLE: REDISPERSED FLY ASH) SINGLE STAGE COLLECTOR FEED

Rm No.	Q_G, m^3/min	u_s, cm/s	u_j, m/s Stage No. 1	2	3	ΔP_{bed}, cm W.C. Stage No. 1	2	3	Bed Ht., cm Stage No. 1	2	3	Mass Flow Rate, g/s Collector (Total)	Gas	Inlet Part. conc., mg/m	Plate No. Stage 1	2	3	Electrostatic Conditions
10/P9	0.18	36.2	22.6	22.6	22.6	8.4	8.4	8.4	1.5	1.5	1.5	3.3	3.5	991	D	D	D	CP/PC
10/P10	0.18	36.2	22.6	22.6	22.6	8.4	8.4	8.4	1.5	1.5	1.5	3.3	3.5	2,018	D	D	D	CP/PC
10/P11	0.18	36.2	22.6	22.6	22.6	8.4	8.4	8.4	1.5	1.5	1.5	3.3	3.5	2,337	D	D	D	UP/NC
10/P12	0.23	48.0	19.2	19.2	19.2	6.6	6.9	7.1	1.5	1.5	1.5	1.6	4.7	610	G	G	G	CP/PC
10/P13	0.23	48.0	19.2	19.2	19.2	6.6	6.9	7.6	1.5	1.5	1.5	1.6	4.7	570	G	G	G	CP/PC
10/P14	0.23	48.0	19.2	19.2	19.2	6.6	6.9	7.6	1.5	1.5	1.5	1.6	4.7	1,993	G	G	G	UP/NC
10/P15	0.23	48.0	19.2	19.2	19.2	6.6	6.9	8.0	1.5	1.5	1.5	1.6	4.7	2,308	G	G	G	UP/NC
10/P16	0.22	44.5	17.8	17.8	17.8	5.6	6.0	6.4	1.5	1.5	1.5	1.6	4.4	300	G	G	G	CP/PC
10/P17	0.22	44.5	17.8	17.8	17.8	5.6	6.0	6.4	1.5	1.5	1.5	1.6	4.4	464	G	G	G	CP/PC
10/P18	0.22	44.5	17.8	17.8	17.8	5.6	6.0	6.4	1.5	1.5	1.5	1.6	4.4	1,999	G	G	G	UP/NC
10/P19	0.22	44.5	17.8	17.8	17.8	5.8	6.0	6.4	1.5	1.5	1.5	3.3	4.4	1,921	G	G	G	UP/NC
10/P20	0.22	44.5	17.8	17.8	17.8	5.8	6.0	6.4	1.5	1.5	1.5	3.3	4.4	2,069	G	G	G	UP/NC
10/P21	0.22	44.5	17.8	17.8	17.8	5.8	6.0	6.4	1.5	1.5	1.5	3.3	4.4	596	G	G	G	CP/PC
10/P22	0.22	44.5	17.8	17.8	17.8	5.8	6.0	6.4	1.5	1.5	1.5	3.3	4.4	582	G	G	G	CP/PC
10/P23	0.22	44.5	17.8	17.8	17.8	5.8	6.0	6.4	1.5	1.5	1.5	3.3	4.4	2,370	G	G	G	CP/PC
10/P24	0.22	44.5	17.8	17.8	17.8	5.8	6.0	6.4	1.5	1.5	1.5	3.3	4.4	2,229	G	G	G	UP/NC
10/P25	0.22	44.5	17.8	17.8	----	6.0	6.4	---	1.5	1.5	---	---	4.4	571	G	G	-	CP/PC
11/P1	0.22	44.5	17.8	17.8	----	6.0	6.4	---	1.5	1.5	---	3.3	4.4	1,340	G	G	-	CP/PC
11/P2	0.22	44.5	17.8	17.8	----	6.0	6.4	---	1.5	1.5	---	3.3	4.4	998	G	G	-	CP/PC

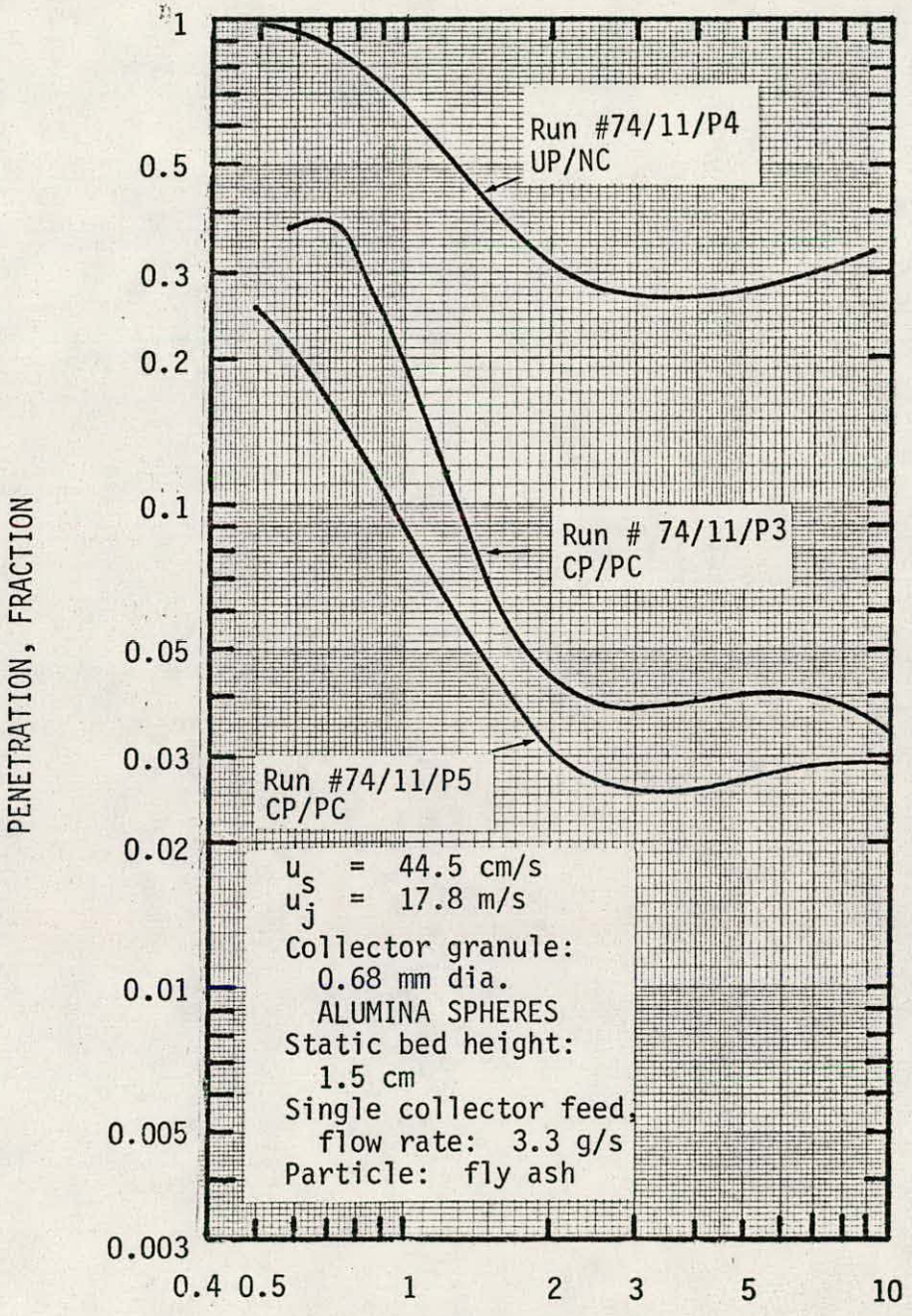

Figure 9. Comparison of one-stage performance for DPS and EDPS.

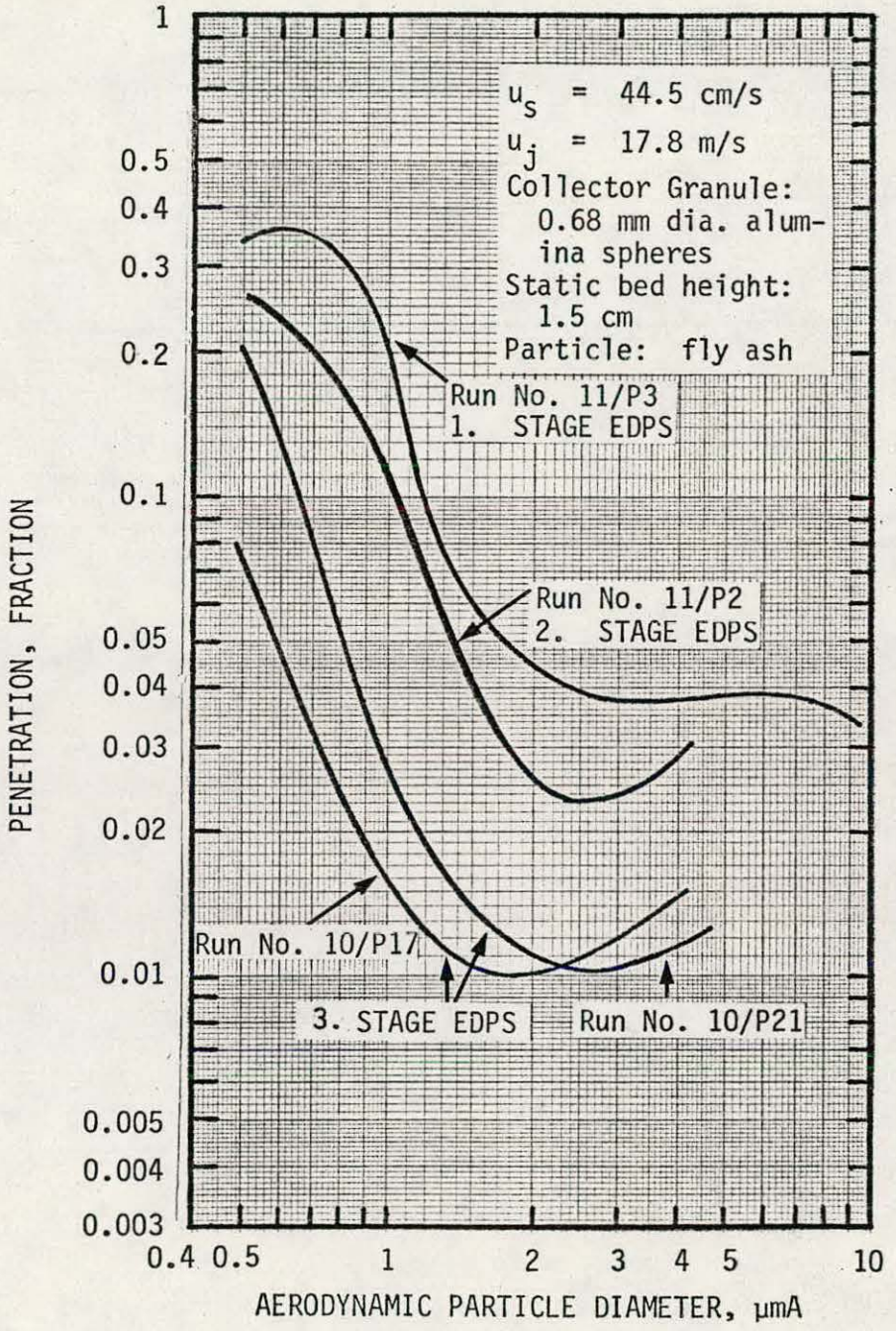

Figure 10. Measured 1-, 2- and 3-stage continuous EDPS performance.

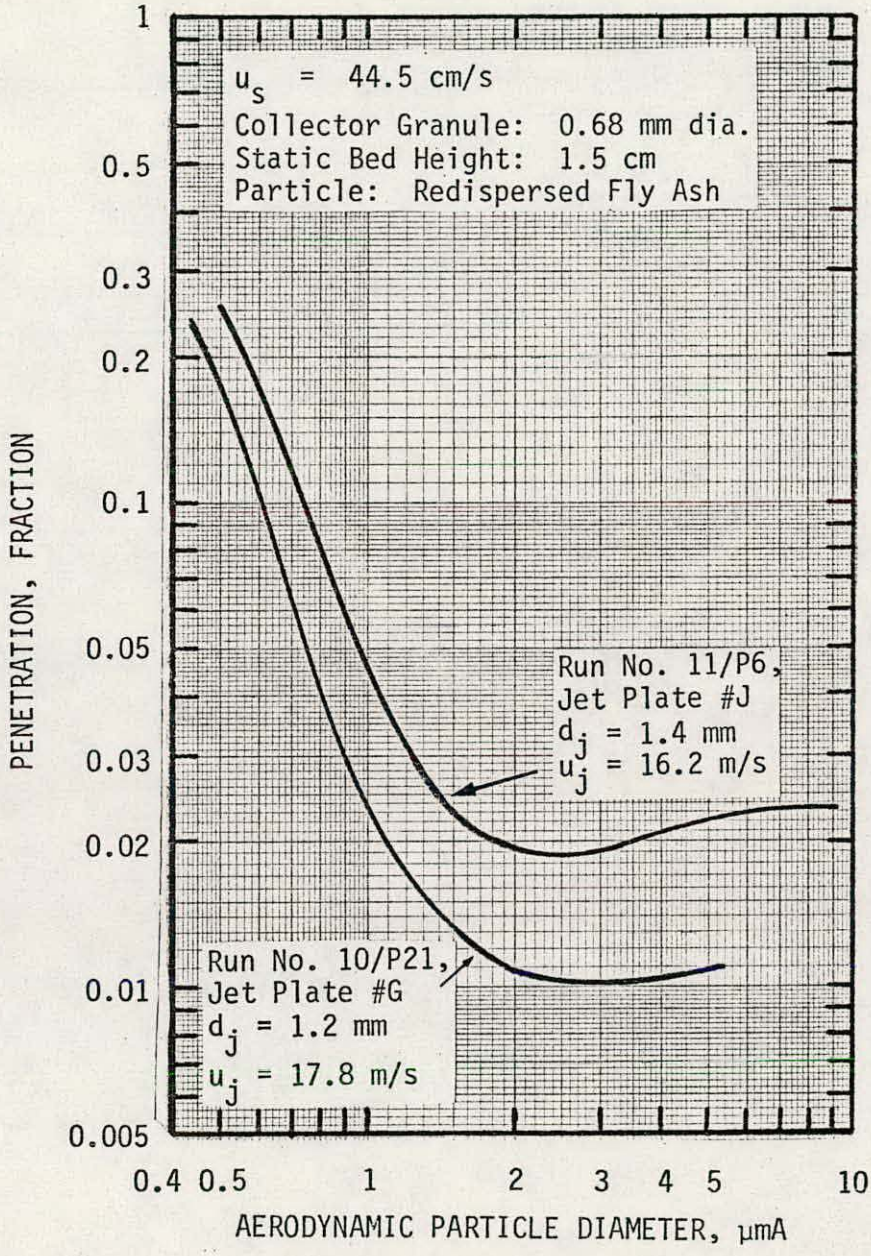

Figure 11. Combined effect of EDPS jet diameter and jet velocity.

Figure 13 compares measured grade penetration data for zirconia beads and alumina spheres on the EDPS system. Zirconia beads achieve better efficiency, at 55% increase in gas capacity, particularly for large particles greater than 1.5 μmA. No problem of attrition with these larger size of zirconia beads was seen. Earlier zirconia beads of size 0.3 - 0.6 mm diameter were observed to break up by attrition in the bed as they were reused.

Electrical Conductivity Experiments

Measurement apparatus was built to measure the electrical conductivity of a bed of alumina spheres at various temperatures.

Two parallel electrodes were suspended in the bed. A 1,000 V source was available to momentarily connect to one electrode. A sensitive electrometer was connected to the other to monitor leakage current through the bed which could be converted into total resistance of the bed.

Figure 14 presents the electrical conductivity (or resistivity) data for an alumina sphere bed. The figure shows resistivity data for the clean alumina bed, and alumina bed saturated with Curtiss-Wright PFBC fly ash. Also technical data for standard ESP solid alumina insulator supplied by Coors Co. are presented. It is noted that at about 800°C, the electrical resistivity of the alumina bed is about 10^5 - 10^6 Ω-cm. This is much more conductive than a room temperature bed, but much less conductive than a perfect (metal) conductor.

Required Performance

The particle removal performance requirement for a Dry Plate Scrubber depends on the intended use of the cleaned gas. If it is to be passed through a gas turbine, the gas should meet the turbine cleaning requirement. The maximum allowable particle concentration in the gas for the gas turbine has been estimated to be 0.023 g/DNm³. From this maximum allowable particle concentration, one can predict the performance requirement for any control

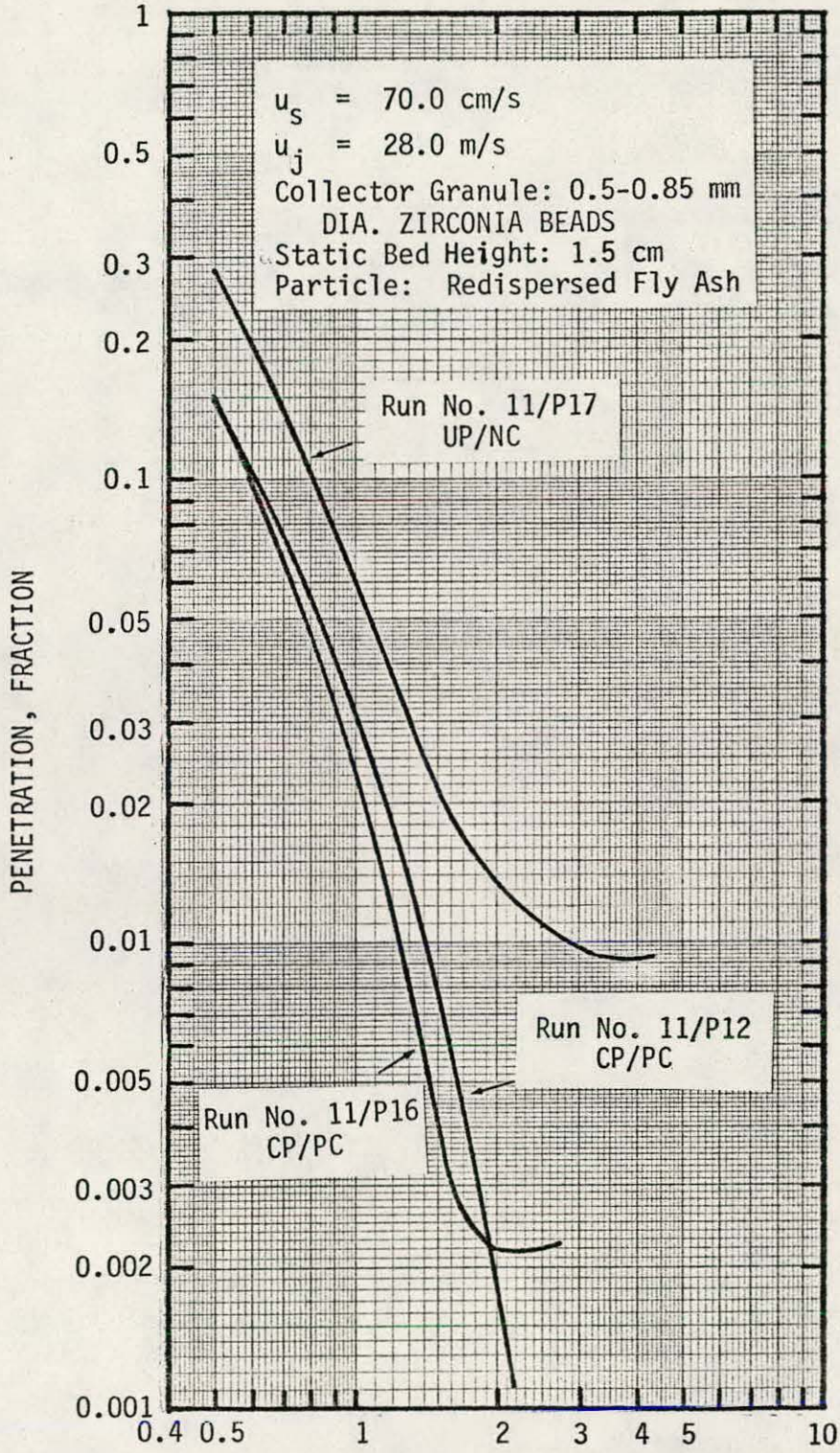

Figure 12. Measured three-stage continuous EDPS performance with and without electrostatic augmentation.

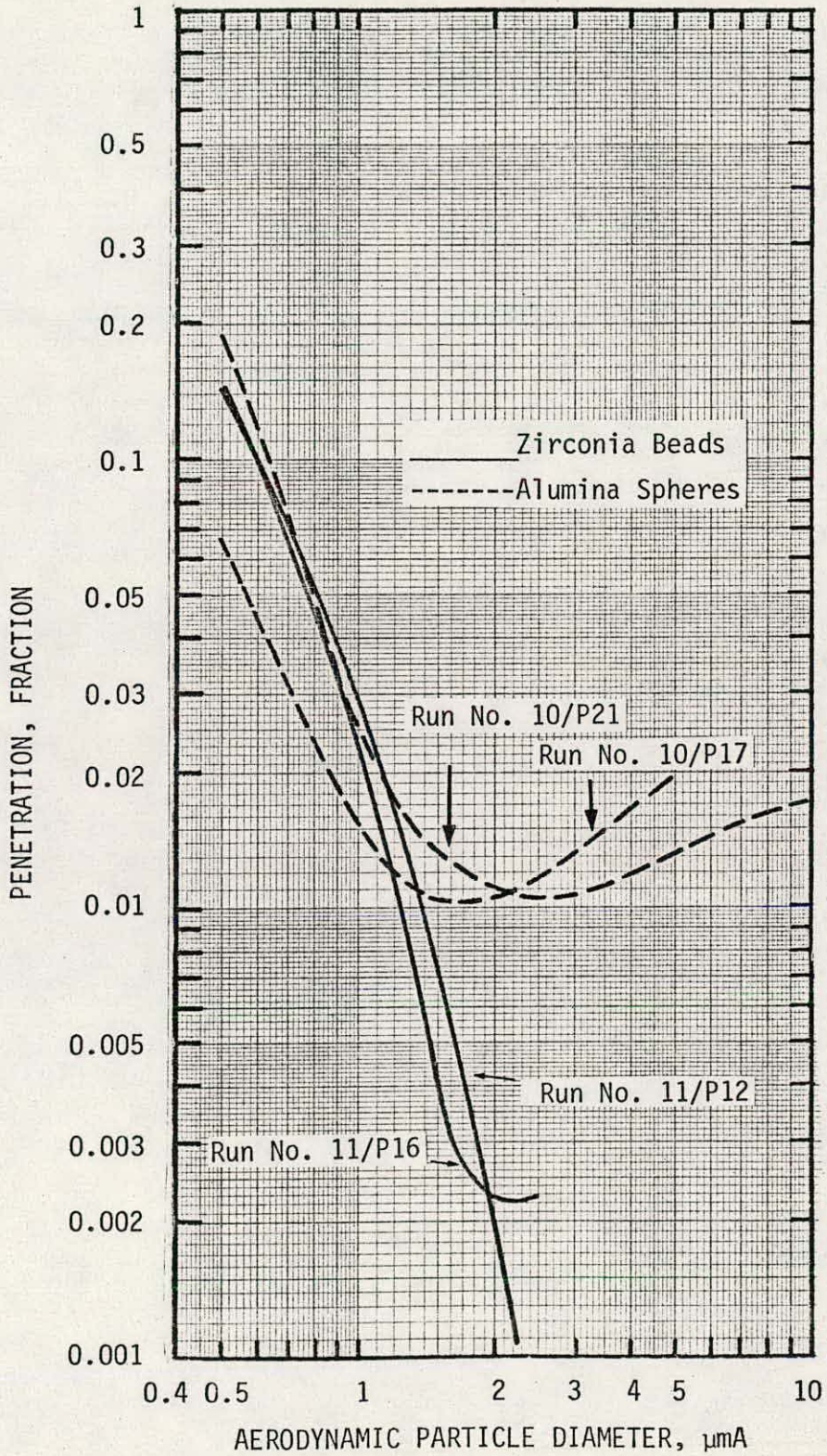

Figure 13. Comparison of EDPS performance between alumina spheres and zirconia beads as collectors.

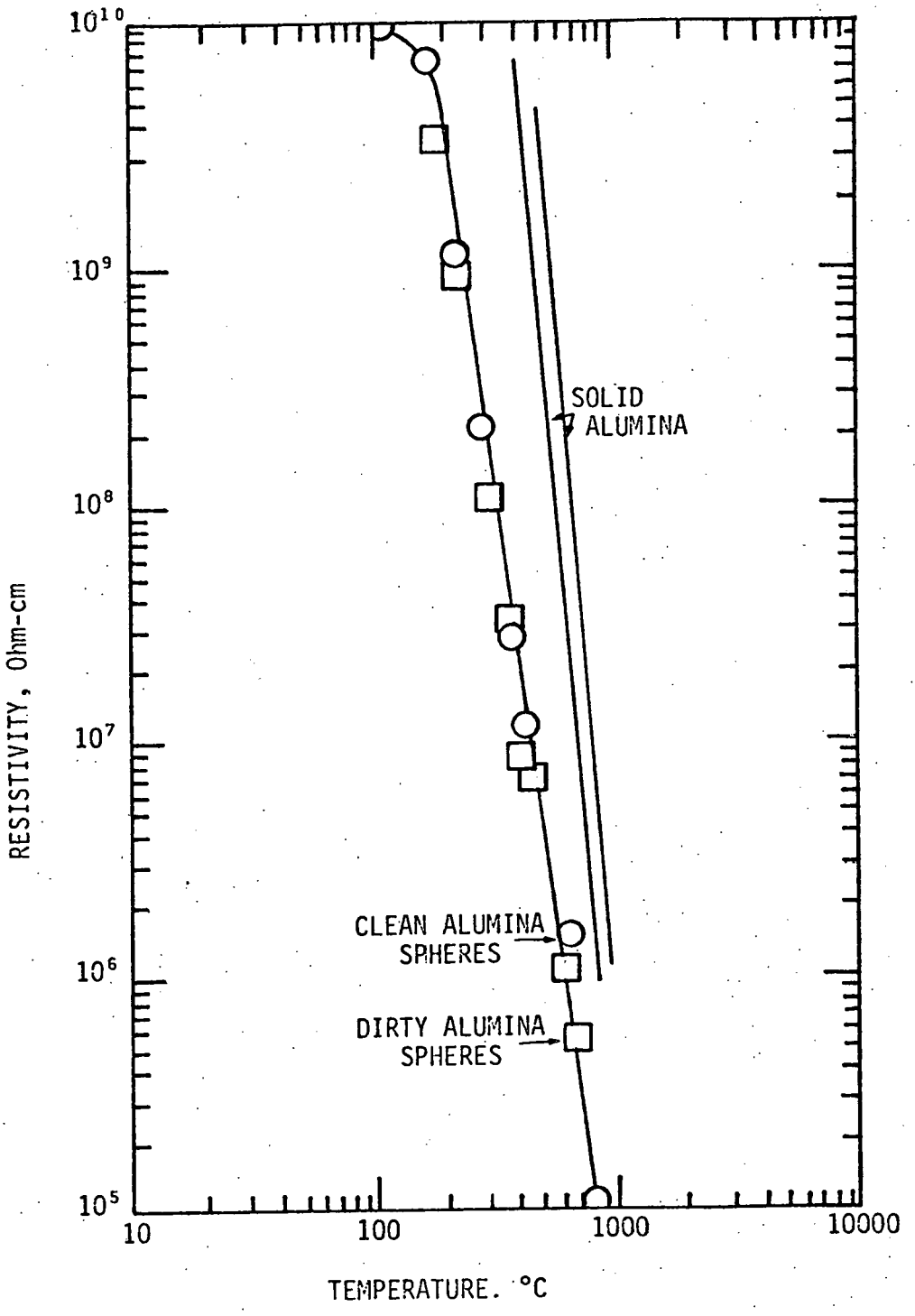

Figure 14. Resistivity data for alumina bed.

device if the inlet particle size distribution is known.

Hoke, et al. (1980) reported some particle size distribution data for the Exxon PFBC miniplant. The average mass median particle diameter was shown to be about 6.8 μmA and the geometric standard deviation about 3. The particle concentration varies with the coal type and operation of the FBC. Typical values are expected to fall within the range 0.23-2.3 g/DNm^3.

Using the information by Hoke, et al. (1980) and the maximum allowable particle concentration of 0.023 g/DNm^3, the estimated allowable penetration for a control device ranges from 0.01 to 0.1; i.e., 1% to 10%. The grade penetration curve required to achieve the required overall penetration can be estimated by the use of cut/power design method (Calvert, 1974). The cut/power prediction was based on the assumption that penetration varies with $\exp -(-d^2_{pa})$. Figure 15 shows the predicted required grade penetration curves to achieve overall penetrations of 0.01 and 0.1. Based on information from the original DOE PRDA, the required overall penetration for 0-5 μmA diameter particles is 0.019 to 0.19.

The dashed lines in Figure 15 represent the EDPS performance data. The overall penetrations for the two runs shown in Figure 15 were predicted by graphical integration. Assuming the same PFBC fly ash size distribution as above, we get overall penetrations of 0.015 to 0.021 for the EDPS. Therefore, the EDPS meets the most stringent cleanup requirement for 0-5 μmA particles.

TASK 3.1 - SORBENT SCREENING EXPERIMENTS

Sorbent screening experiments were run and the analysis was completed this quarter. Thirteen sorbents were screened. They are listed in Table 8. All the screening runs were conducted in a fixed bed with a superficial bed velocity of 51 cm/s and a gas space velocity of 10/s in a fixed bed with a superficial bed velocity of 51 cm/s and a 0.1 s contact time. The sodium chloride vapor was maintained at 40 ppm. The bed temperature was kept at 790°C. The operating conditions for the sorbent screening runs are given in Table 9.

The amount of sodium chloride vapor captured by the sorbent was

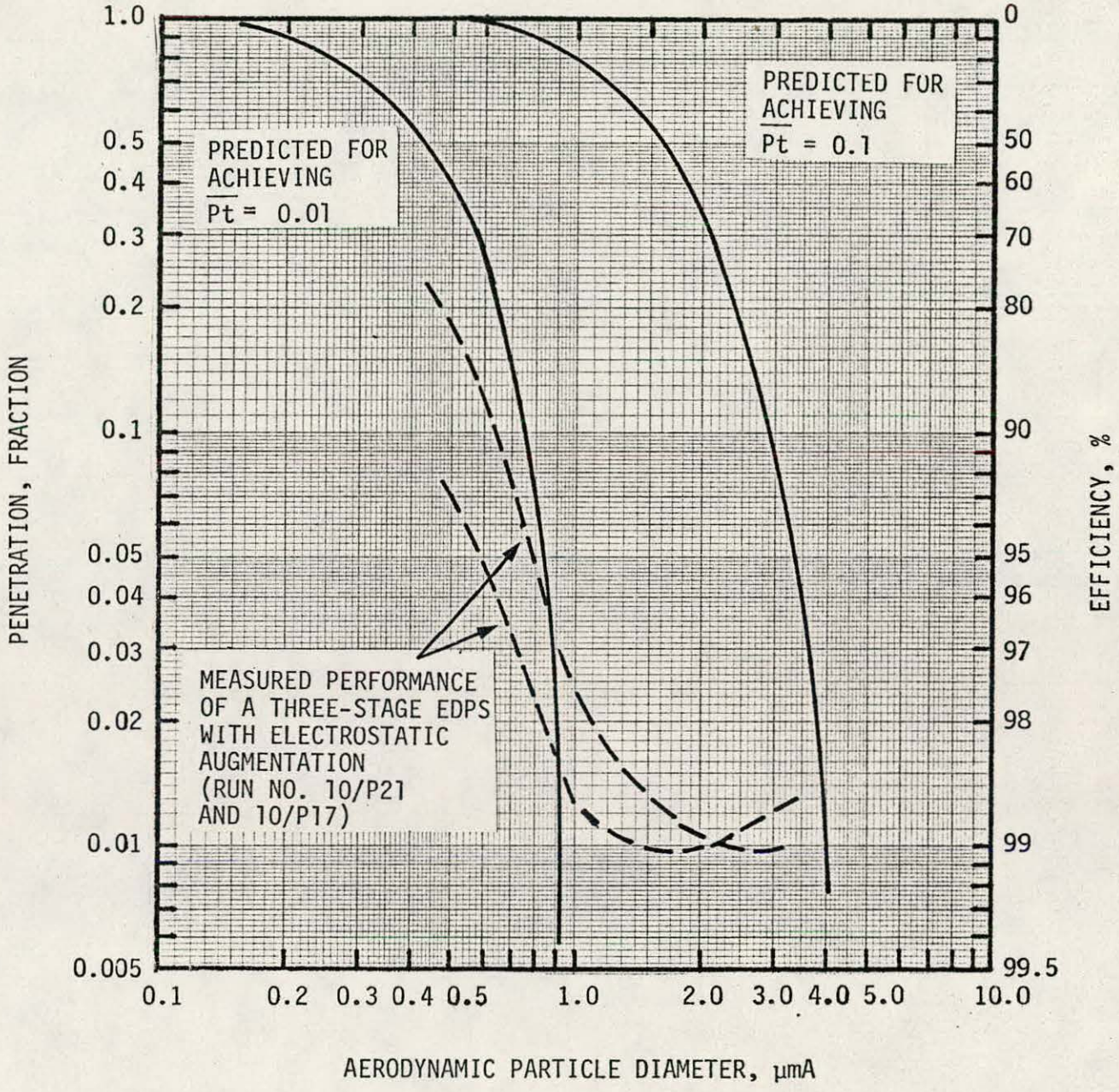

Figure 15. Predicted performance requirement and measured performance for an EDPS.

obtained by direct analysis of the sodium content of the sorbent. To determine the sodium content of the sorbent, the granules were ground, mixed and a representative sample of approximately 0.6 g completely dissolved in a suitable acid. Table 10 lists the dissolving techniques for the sorbents analyzed. The sodium concentration of the acid solution was then obtained by atomic absorption spectroscopy.

Four sorbents (Alumina, Norton Catalysts SA5201 and SA6190, and Fuller's Earth) could not be dissolved completely by these techniques. Therefore, in these cases the total sodium uptake could not be determined. Instead, the amount of physically absorbed sodium was determined by leaching the samples with water at about 90°C for 0.5 hr. The solution was then analyzed with a specific ion electrode. Table 11 shows the amount of physically absorbed sodium by these four sorbents. It can be seen that the amount absorbed is small.

Figures 16 and 17 show the amount of NaCl captured per gram of sorbent and per unit volume of sorbent bed plotted against the experiment duration, respectively. As can be seen, the amount of NaCl captured by diatomaceous earth is substantially greater than that by other sorbents. For this reason, diatomaceous earth is chosen for further study. Experiments for determining its sorption capacity and efficiency are in progress.

TASK 3.2 - SORPTION RATE AND EFFICIENCY EXPERIMENTS

The sorption rate experiments are being conducted in the laboratory scale single stage DPS. The purpose of the rate experiments is to establish the sorbent size and type, bed thickness, sorbent feed rate, and gas flow rate for maximum alkali vapor removal at 900°C.

A schematic diagram of the apparatus is shown in Figure 18. Incoming air atomizes water to form a fine aerosol. The air is then heated electrically to vaporize the water. The hot air stream is mixed with fine NaCl aerosol from an atomizer, and passed through a high temperature furnace to vaporize the NaCl. The hot gas then enters the vertical test section. A bed of alumina spheres is used to promote good mixing before the inlet sample point. The gas passes through the sorbent bed, which may be still or

Table 8. List of Sorvents Evaluated

Sorbent	Major Composition	Source
1. Diatomaceous Earth (Celatom MP91)	SiO_2(92%), Al_2O_3(5%)	Eagle Picher Industries
2. Diatomaceous Earth (Celatom MP94)	SiO_2(92%), Al_2O_3(5%)	Eagle Picher Industries
3. Diatomaceous Earth (Celatom MP99)	SiO_2(92%), Al_2O_3(5%)	Eagle Picher Industries
4. Activated Bauxite (Driocel)	Al_2O_3(81%), SiO_2(10%)	Engelhard Minerals & Chemical Co.
5. Activated Bauxite (High Alumina)	$Al_2^2O_3$(88%), SiO_2(7%)	Engelhard Minerals & Chemical Co.
6. Attapulgous Clay	SiO_2(68%), Al_2O_3(12%, MgO(10%)	Engelhard Minerals & Chemical Co.
7. Fuller's Earth	SiO_2(66%), Al_2O_3(12%), Fe_2O_3(4%)	Floridin Co.
8. Silica Gel	SiO_2	Philadelphia Quartz Co.
9. Dolomite	$CaCO_3$(56%), $MgCO_3$(42%)	Kaiser Industries
10. Calcined Dolomite	CaO, MgO	Kaiser Industries
11. Norton Catalyst SA 5201	Al_2O_3(80-90%), SiO_2(5-10%)	Norton Co.
12. Norton Catalyst SA 6190	Al_2O_3(80-90%), SiO_2(5-10%)	Norton Co.
13. Alumina	Al_2O_3	Ferro Corp.

Table 9. Sorbent Evaluation:
Operating Conditions

OPERATING CONDITIONS

Bed superficial vel., cm/s =	51	Bed diameter, cm	= 6
Bed contact time, sec.	0.1	Sorption temp., C	= 790
Bed depth, cm	5.1	NaCl vapor conc., ppm(wt)	= 40

RUN #	SORBENT	SORPTION TIME, HRS.
8/S4	Diatomaceous Earth (MP-91)	2
9/S1	Activated bauxite (Driocel)	2
9/S2	Activated bauxite (Driocel)	3
9/S3	Attapulgous clay	2
9/S4	Attapulgous clay	3
9/S5	Alumina	2
9/S6	Alumina	3
9/S7	Dolomite (Kaiser)	3
9/S8	Dolomite (Kaiser)	2
9/S9	Silica Gel	3
9/S10	Norton Catalyst SA 5201	2
9/S11	Norton Catalyst SA 5201	3
9/S12	Silica Gel	2
9/S13	Norton Catalyst SA 6190	3
9/S14	Dolomite (Kaiser)	2
9/S15	Diatomaceous Earth (MP 99)	2½
9/S16	Activated bauxite (High alumina)	2
9/S17	Diatomaceous Earth (MP 99)	2
9/S18	Activated bauxite (High alumina)	3
9/S19	Fuller's Earth (Florex)	2
9/S21	Diatomaceous Earth (MP 94)	1¼
9/S22	Diatomaceous Earth (MP 94)	2
9/S23	Diatomaceous Earth (MP 91)	2
9/S24	Calcined Dolomite	2

Table 10. Solvents for Sorbent Analysis

SORBENT	DISSOLVING ACID
1. Diatomaceous Earth (MP 91, 94, 99)	Hot HF, H_3BO_3 mixture
2. Dolomite	Hot HCl
3. Activated Bauxite (Driocel)	Pressure digestion with HF 26
4. Attapulgous Clay	Hot HF, H_3BO_3 mixture

Table 11. Amount of Physically Absorbed Sodium

Run#	Sorbent	Sorption Duration Hrs.	Amount of Sodium* Physically Absorbed mg/g sorbent
74/9/S5	Alumina	2	< 0.01
74/9/S6	Alumina	3	< 0.01
74/9/S10	Norton Catalyst SA5201	2	< 0.01
74/9/S11	- do -	3	< 0.01
74/9/S13	Norton Catalyst SA6190	3	0.02
74/9/S19	Fuller's Earth (Florex)	2	0.07

*Obtained by leaching sorbent sample with hot water (~90°C) for half an hour. The leach was then analyzed for sodium content with Orion sodium electrode.

It was not possible to dissolve any of the above sorbents completely in hot and concentrated HF, HNO_3, HCl & H_3BO_3. So the total amount of sodium taken up by the sorbents was not determined.

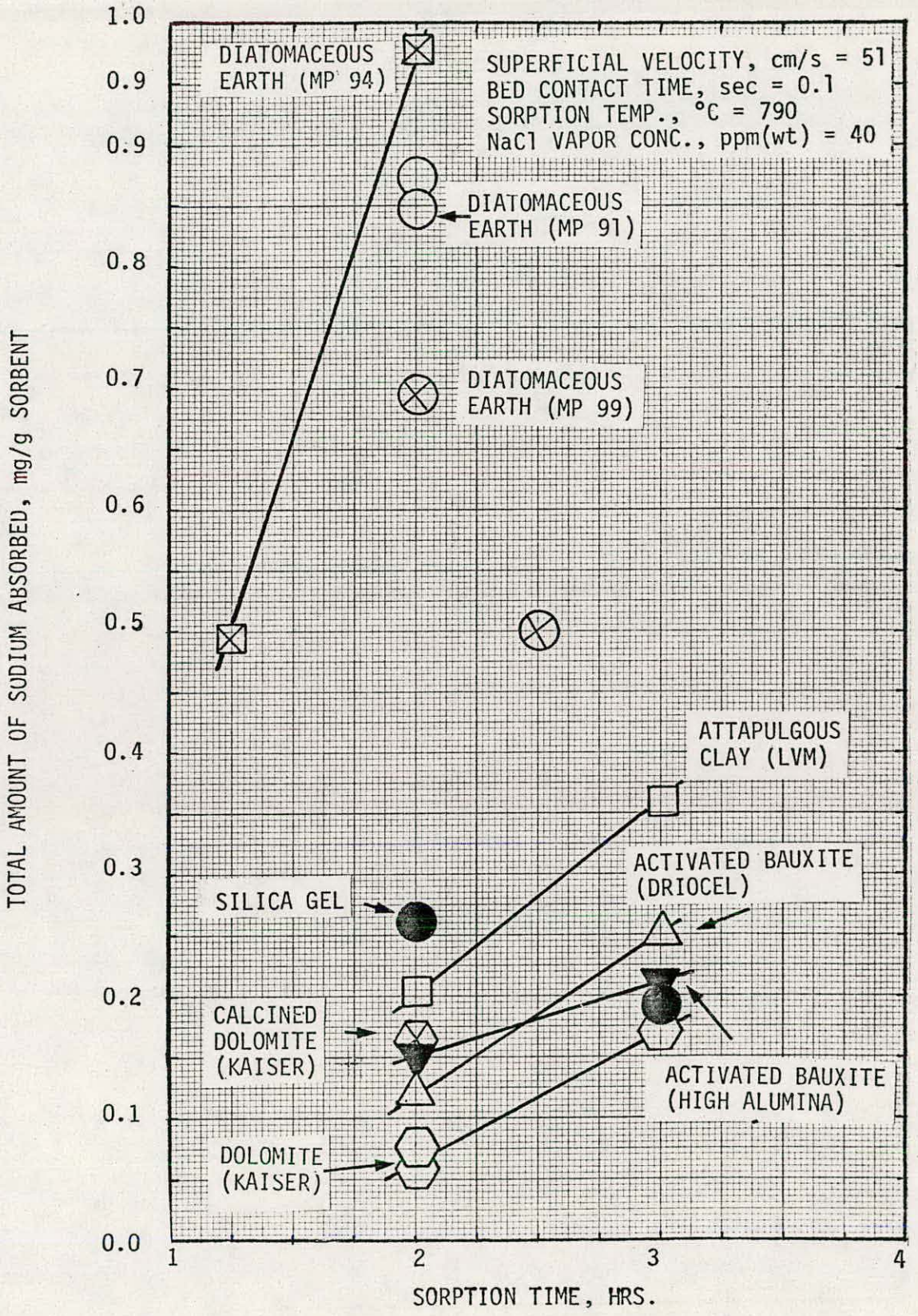

Figure 16. Sodium absorption - sorbent screening runs.

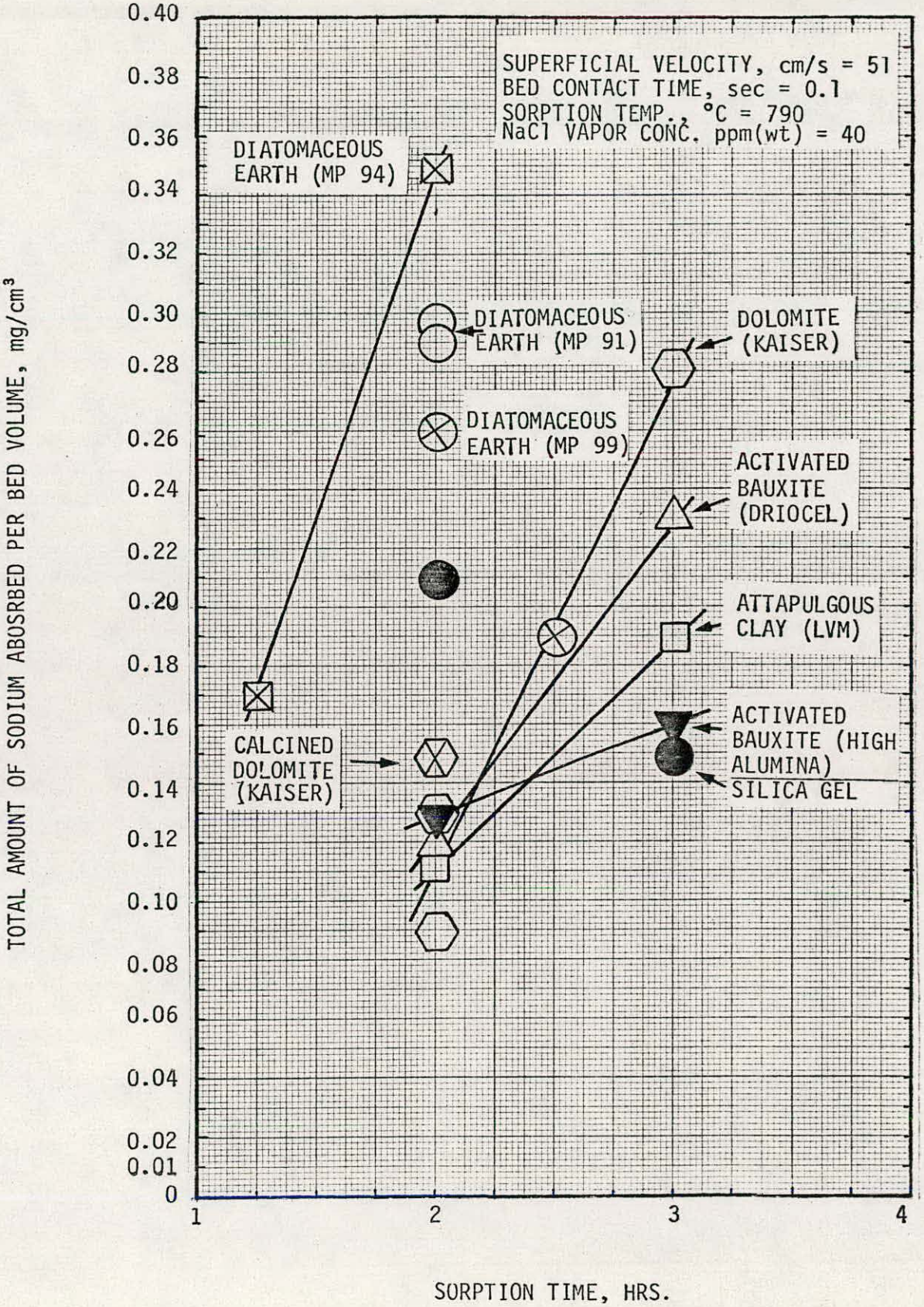

Figure 17. Sodium absorption - sorbent screening runs.

fluidized, and out through a cooling section and a final filter.

Two sampling methods are used. In the first method, a sample is withdrawn through a cold trap to condense the NaCl vapor and a pretreated quartz filter to collect the condensed NaCl particles which penetrate the cold trap. The filter and cold trap is then washed with distilled, de-ionized water. The water is analyzed for NaCl with specific ion electrodes.

Pretreatment of the quartz filter is done by heating the fresh filter in a flowing air stream at aroung 400°C for about 12 hours to eliminate volatile impurities. The filter is then cooled, washed in an ultrasonic bath and finally dried before use.

Inlet and outlet samples were collected simultaneously. The NaCl vapor concentrations and the bed capture efficiency are calculated by the following method.

(1) From the wash volume and the salt concentrations as detected by the specific ion electrodes, calculate weights of sodium and chloride collected in the cold trap and filter.

(2) Determine the total air volume that is sampled (from gas meter in the sampling train).

(3) Vapor concentration of Na^+ or Cl^- =

$$= \frac{\text{total collected weight of } Na^+ \text{ or } Cl^-}{\text{sample volume}}$$

(4) Bed capture efficiency = $\frac{1 - \text{vapor concentration at outlet}}{\text{vapor concentration at inlet}} \times 100\%$

Diatomaceous earth (MP-94) was the first sorbent chosen to be tested because the screening experiments showed this sorbent to be the most effective for sodium capture at 800°C when the sorbent is pretreated at around 800°C in flowing air for about 2 hours. The rate experiments will also be done with the other two promising sorbents--activated bauxite and dolomite.

Alumina and zirconia are the two most promising collectors for particle capture. Sorption runs will also be done with these two materials to determine their alkali capture efficiency.

Two runs with diatomaceous earth (MP-94) have been completed. The inlet and outlet samples are currently being analyzed. The results will be

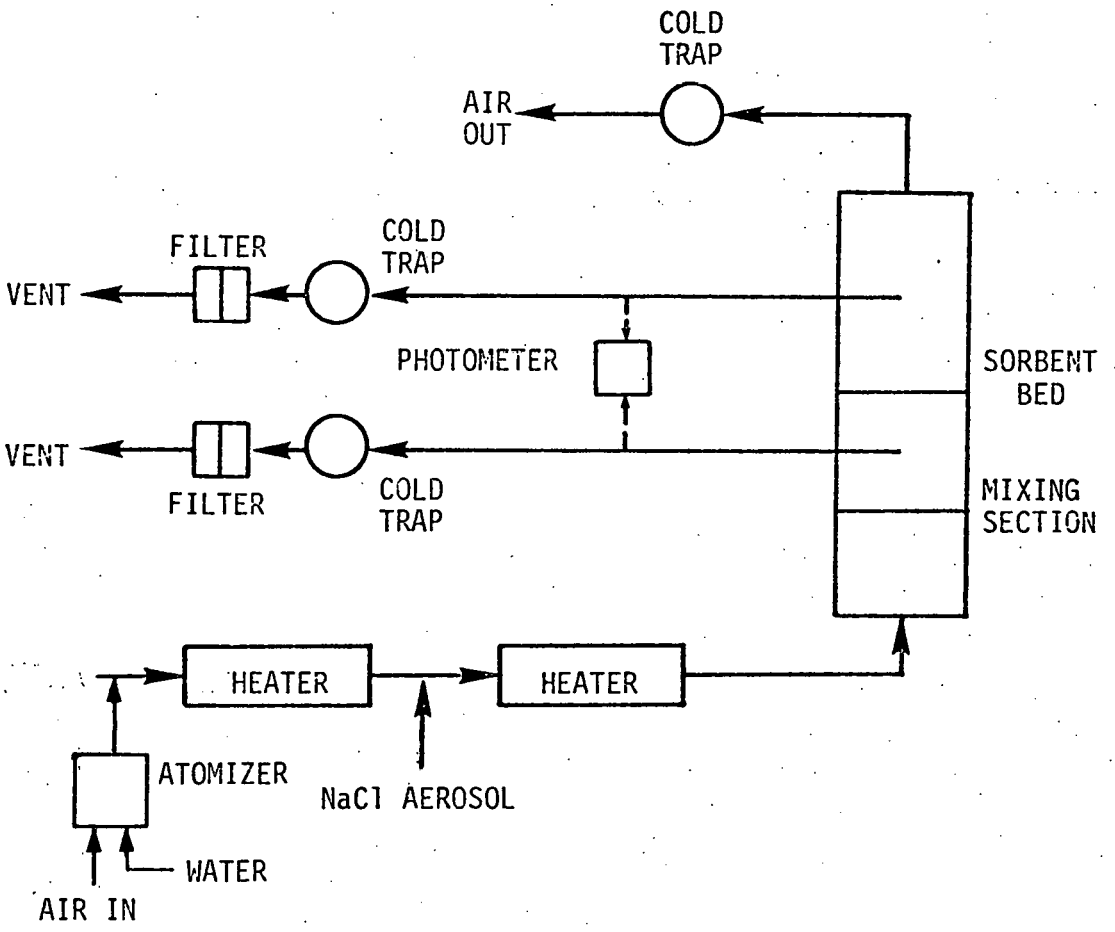

Figure 18. Laboratory-scale single stage DPS.

reported in the next progress report.

Pretreatment of Sorbents

The purpose of the pretreatment is to enhance sorbent performance. At present, sorbent samples are pretreated physically by heating them in flowing air at 1,000°C for about 15 hours. Chemical pretreatment is also being investigated. The objectives of chemical pretreatment are to open the pores in the sorbent and to introduce constituents in the pores.

Activated bauxite and diatomaceous earth (MP-94) will be chemically pretreated with sodium hydroxide and boron oxide.

Pretreated sorbents will then be used for sorption experiments in the single stage high temperature DPS.

Flame Photometer

The flame photometer was modified for high temperature sampling of sodium chloride vapor.

The modified system was tested with hot air containing NaCl vapor. A continuously drifting response was observed. The output of the photometer is very sensitive to the temperatures of the photomultiplier tube and the incoming hot air stream. The latter probably affects the flame temperature. Light emission from the flame is known to be very sensitive to the flame temperature.

Sampling with hot air presents another problem. Sorption runs will be conducted over a range of bed superficial velocities. So the air flow rate through the bed and into the photometer will vary. Stable operation of the burner over a range of air flow rates is doubtful. Repeated calibration will also be necessary with varying air flow rates.

Due to these problems we are designing a sample dilution system. The purpose of the dilution air is 1) to cool the air stream without depositing NaCl on the tube walls, and 2) to provide a constant air flow rate to the burner.

TASK 4.1 - HIGH TEMPERATURE AND PRESSURE BENCH SCALE DPS

HTP System Design

The conceptual design for bench scale high temperature and pressure (HTP) DPS has been completed. The detailed process design, material and energy balances, equipment specifications, selection and ordering are being carried out. The conceptual design is discussed briefly below. A schematic diagram of the bench scale HTP Dry Plate Scrubber is presented in Figure 19.

The design is a once-through passage of hot gas with multiple particle collection stages and one or more alkali sorption stages. Air will be compressed to about 20 atmosphere pressure. Part of the compressed air will be used to redisperse PFBC fly ash. Another part will be used for producing liquid NaCl aerosols which will be evaporated to form NaCl vapor.

The collector granules will be fed from a lock hopper to the DPS at the top and removed from the bottom. The granules will be heated by a stream of hot clean air by direct contact. Alkali vapor and fly ash particles will be collected by the granules in the DPS.

The air streams will be electrically heated to 900°C before entering the vertical DPS. The hot exhaust air stream from the DPS will be used to preheat the incoming air.

The DPS itself will be enclosed in a pressurized vessel. Inlet and outlet samples will be drawn isokinetically for particulate and vapor concentration measurements.

Downcomer Study Experiments

Flow of collectors from stage to stage in a multiple stage DPS takes place through downcomers. The steady state operation of DPS requires continuous removal of dirty collectors and feeding of clean collectors.

The purpose of these experiments is to obtain the best design for downcomers so that the DPS will operate at steady state in a wide range of operating conditions. The results of these experiments will be used for detailed mechanical design of the bench-scale DPS.

The downcomer experiments are being carried out in a 3-stage DPS column which is made of Plexiglass for visual observations. Column diameter is 23 cm (8 in.) and supporting plates are of the plate "G" design (Table 4). Figure 20 shows the experimental set-up. Experiments are in progress. Results will be presented in the next progress report.

TASK 4.3 - BENCH SCALE TESTS ON AFBC SYSTEM

AFBC System Design

Atmospheric Fluidized Bed Combustor Process Design

We will test the DPS on an atmospheric fluidized bed combustor (AFBC) first instead of operating the DPS at high pressure as originally planned. The main reason for this change is that it offers an immediate study of potential plugging problems. Figure 21 presents a process flow sheet of the AFBC plant. It was designed for a flue gas flow rate of 14.2 Am^3/min (500 ACFM) at 820°C. A brief description of the combustor is given below.

A positive displacement blower provides fluidizing air at 130 kPa delivery pressure. This blower provides constant volume output under varying operating conditions. The combustor is preheated to coal ignition temperature (~700°C) by burning natural gas. The combustor is a 45 cm (18 in.) diameter carbon steel vessel lined with 7.5 cm (3.0 in.) thick castable ceramic (Grefco 75-28 litecast refractory), i.e., the actual internal diameter of the combustor is 30.0 cm. The gas distribution grid is a perforated Inconel-600 plate with a square grid design (0.16 cm holes on 1.0 cm centers).

The combustion gas is ducted through a crossover duct to a conventional cyclone. The cyclone collects fly ash particles larger than about 10-15 μmA diameter. Diverter valves made of 347 SS are installed in the cyclone exit duct to divert a side stream to the DPS. The main stream goes through a quencher, which cools the gas and removes large particles before entering a Venturi scrubber for final cleaning of the gas stream. There is an exit blower to move the gas through the Venturi. The combustor is fully equipped with necessary instrumentation, control and safety equipment.

BENCH SCALE H.T.P. SYSTEM PROCESS DESIGN

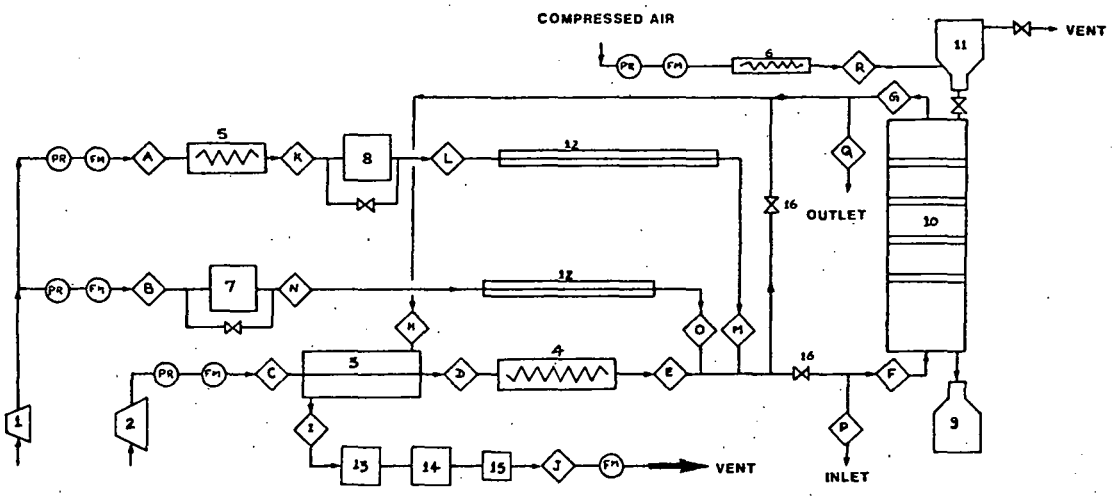

PROCESS CONDITIONS

STREAM No.	TEMP., °C	PRESSURE, Psig	FLOW RATE, ACFM	FLOW RATE, SCFM	GAS DENSITY, #/ft³	MASS FLOW RATE, lb/min.
A	27	275	1.0	19.7	1.44	1.4
B	27	175	1.0	12.9	0.94	0.9
C	27	135	4.7	48.2	0.74	3.5
D	500	135	12.2	48.2	0.29	3.5
E	995	135	20.0	48.2	0.18	3.5
F	900	135	30.0	78.2	0.19	5.7
G	900	130	31.0	78.2	0.18	5.7
H	850	130	28.7	75.7	0.19	5.5
I	550	130	21.1	75.7	0.26	5.5
J	27	0	75.7	75.7	0.07	5.5
K	300	275	1.9	19.7	0.76	1.4
L	250	135	3.4	19.7	0.43	1.4
M	700	135	6.3	19.7	0.23	1.4
N	27	135	1.3	12.9	0.74	0.9
O	700	135	4.1	12.9	0.23	0.9
P_{INLET}	900	135	1.0	2.6	0.19	0.2
Q_{OUTLET}	900	130	1.0	2.5	0.18	0.2
R	900	135	0.5	1.3	0.19	0.1

MAJOR SYSTEM COMPONENTS

EQUIPMENT No.	IDENTIFICATION	FUNCTIONS AND REQUIREMENTS
1	COMPRESSOR	SUPPLY AIR AT 40 SCFM @ 275 PSIG TO RUN ATOMIZER AND DUST GENERATOR.
2	COMPRESSOR	SUPPLY AIR AT 50 SCFM @ 140 PSIG TO MAKEUP SYSTEM CAPACITY. (PREFERRED 80-90 SCFM).
3	RECUPERATIVE HEAT EXCHANGER	RECOVER HEAT FROM DPS EXHAUST GASES AND UTILIZE THAT TO HEAT INCOMING GAS. (300°C)
4	DIRECT HEATER	HEAT AIR FROM H.E (1KW) TO RAISE TEMP. TO ABOUT 1000°C.
5	DIRECT HEATER	HEAT AIR TO ABOUT 300°C (1.0 ACFM @ 275 PSIG) BEFORE SENDING TO DUST GENERATOR.
6	DIRECT HEATER	HEAT 0.5 ACFM @ 135 PSIG TO ABOUT 900°C FOR HEATING COLLECTORS BY DIRECT CONTACT.
7	H.P. ATOMIZER	ATOMIZE NaCl SOLUTION TO PRODUCE 13.26 mg/m³ SOD. CHLORIDE VAPOR (5-10 PPM BY WEIGHT)
8	DUST GENERATOR	TO PRODUCE 2.5-3.5 g/min DUST @ 135 PSIG.
9	COLLECTOR HOPPER	TO RECEIVE COLLECTORS FROM DPS @ 135 PSIG.
10	D. P. S.	THREE - PARTICLE COLLECTION STAGES (WITH ONE HEATED ELECTROSTATIC AUX.) + ONE SORBENT BED.
11	LOCK HOPPER	TO STORE COLLECTORS @ 900°C, 130 PSIG FOR TEST.
12	HEATING FURNACES/ TAPES	TO RAISE STREAM TEMP. (DUST & ALKALI) TO 700°C OR MORE. (MAX. 900°C).
13	QUENCHER	TO COOL DOWN GASES FROM D.H.E. TO ABOUT ROOM CONDITIONS.
14	FILTER	TO REMOVE PARTICULATE MATTER PRIOR TO VENTING.
15	PRESSURE LET DOWN	135 PSIG → 0 PSIG.
16	VALVES	FOR BY-PASS LINE (SHOULD) WORK @ 900°C @ 135 PSIG

Figure 19. Bench scale process design for HTP tests.

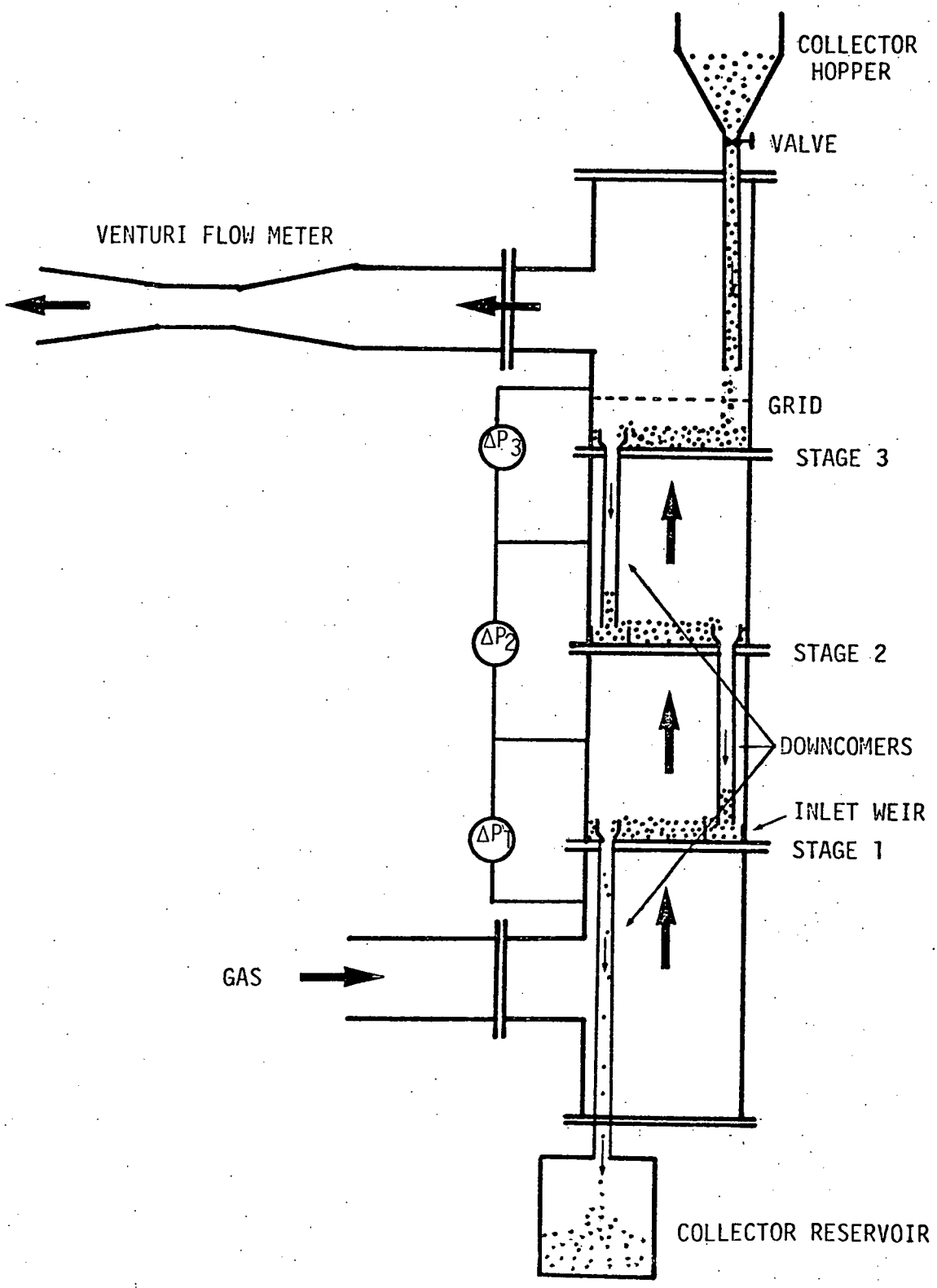

Figure 20. Schematic diagram of downcomer study experimental setup.

AFBC Modification

The combustor diameter will be reduced to 22.5 cm (9.0 in) to reduce the flue gas flow rate to about 7 m^3/min (250 ACFM). About 0.85 m^3/min (30 ACFM) will pass through the DPS.

The AFBC combustor was designed for low sulfur coal and burning coal without absorbent materials. In order to use high sulfur coal with dolomite, the coal feeder will be modified to feed premixed coal and dolomite (Ca/S ratio ≅ 3:1 on mole basis) continuously at a predetermined feed rate.

The freeboard disengagement height of the combustor will be raised to prevent excessive carryover of fine particles and increase residence time in combustor for complete combustion and SO_2 capture.

The combustor will be operated adiabatically at about 150% excess air to remove excess heat of combustion and to maintain the temperature at 870°C (1,600°F).

The AFBC will be tested after these modifications. Any operational problems encountered will be resolved before using the effluents for evaluation of the Dry Plate Scrubber. The particle concentration in the gas will be measured.

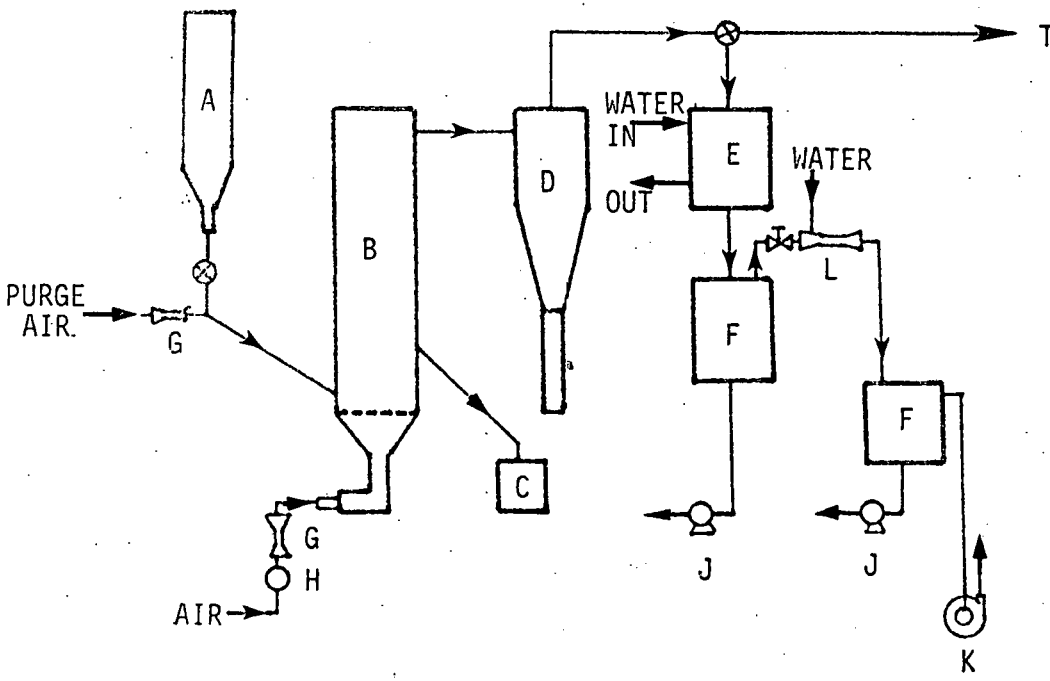

EQUIPMENT DESCRIPTION

A	Coal Feed Hopper
B	Combustor
C	Ash Collection Hopper
D	Cyclone
E	Hot Gas Quencher
F	Entrainment Separator
G	Flow Meter
H	Fluidizing Gas Blower
J	Rotary Discharge Pump (water)
K	Exhaust Blower
L	Venturi Scrubber

Figure 21. Process flow diagram of A.F.B.C. Unit.

REFERENCE

Calvert, S. "Engineering Design of Fine Particle Scrubbers." J. of Air Pollution Control Assoc. 24:929, (1974).

Hoke, R.C. "Miniplant and Bench Studies of Pressurized Fluidized-Bed Coal Combustion." EPA-600/7-80-013, January 1980.